J. Fluid Mech. (1994), *vol.* 280, *pp.* 303–334

The instability of an axisymmetric vortex with monotonic potential vorticity in rotating shallow water

By RUPERT FORD†

Centre for Atmospheric Science, Department of Applied Mathematics and Theoretical Physics, University of Cambridge, Silver Street, Cambridge, CB3 9EW, UK

(Received 28 January 1994 and in revised form 1 July 1994)

The stability of an axisymmetric vortex with a single radial discontinuity in potential vorticity is investigated in rotating shallow water. It is shown analytically that the vortex is always unstable, using the WKBJ method for instabilities with large azimuthal mode number. The analysis reveals that the instability is of mixed type, involving the interaction of a Rossby wave on the boundary of the vortex and a gravity wave beyond the sonic radius. Numerically, it is demonstrated that the growth rate of the instability is generally small, except when the potential vorticity in the vortex is the opposite sign to the background value, in which case it is shown that inertial instability is likely to be stronger than the present instability.

1. Introduction

The appearance of coherent vortical structures in simulations of two-dimensional turbulence, started from random initial conditions, is a familiar phenomenon (Polvani *et al.* 1994; Dritschel 1993; Carnevale *et al.* 1991). Although complex dipolar and tripolar vortical structures have occasionally been observed (e.g. Legras, Santangelo & Benzi 1988), the majority of vortices which form appear to be monopolar, consisting of potential vorticity of one sign only relative to the background value. Moreover, the stripping mechanism suggests that in many cases such vortices will tend to have almost uniform potential vorticity within, and a sharp edge where the potential vorticity changes abruptly (Legras & Dritschel 1993). In any case, a vortex with uniform potential vorticity within and uniform background potential vorticity outside constitutes the simplest possible case for investigation. Since this paper is the first to deal with this instability in rotating shallow water, we shall consider only the simplest cases, and consequently all vortices considered in this paper are of uniform potential vorticity.

Questions have naturally arisen as to the stability of such structures, especially in the case where the basic vortex may be assumed to be axisymmetric. In the case of the two-dimensional Euler equations and the quasi-geostrophic equations, axisymmetric vortices whose potential vorticity varies monotonically with radius can be shown to be both linearly stable and nonlinearly stable in the sense of Arnol'd (Dritschel 1988). However, both the two-dimensional Euler and quasi-geostrophic equations admit only vortical motions, in which knowledge of the potential vorticity field is sufficient to determine uniquely all the other dynamical information. In geophysical fluid dynamics, these equations are generally used as approximate equations for the evolution of the

† Current address: Scripps Institution of Oceanography, 9500 Gilman Drive, La Jolla, CA 92093-0225, USA.

fluid, valid in the asymptotic limits of small Froude number and/or small Rossby number. The full equations of motion in geophysical fluid dynamics admit both inertio-gravity wave and acoustic wave motions in addition to vortical motions (although it may be argued on scaling grounds – see, e.g. Gill (1982) – that the acoustic waves are not significant). It is therefore of interest to investigate the stability of axisymmetric vortices in a system of equations which admit both vortical motions and inertio-gravity waves, and may be studied in the limits of small Froude number and small Rossby number.

The rotating shallow-water equations are the simplest set of equations which admit both vortical motions and inertio-gravity waves, and are thus the simplest set of equations in which the potential vorticity field is not sufficient to determine all the other dynamical information. Axisymmetric vortices of the type described above (i.e. with uniform potential vorticity in their interior) in the rotating shallow-water equations depend on two parameters: the Rossby number Ro, which is characterized by the ratio of the magnitude of the potential vorticity discontinuity at the boundary of the vortex to the background value of potential vorticity, and the Froude number F, which is the ratio of typical velocities in the vortex to the gravity wave phase speed.

A general stability theorem for axisymmetric shallow-water vortices was given by Ripa (1987). It was derived by variational methods, and therefore provides a sufficient condition for stability. The condition is that the axisymmetric flow, with radial coordinate r axisymmetric about $r = 0$, and with azimuthal velocity $V(r)$ and height field $H(r)$, is stable if

$$(V-\lambda r)^2 < H(r), \tag{1}$$

$$(V-\lambda r)\frac{\mathrm{d}Q}{\mathrm{d}r} \geqslant 0, \tag{2}$$

for some λ, where $Q = (f+\mathrm{d}V/\mathrm{d}r + V/r)/H(r)$ is the potential vorticity in the basic state. In the case of an isolated vortex in unbounded shallow water, (1) can only be satisfied if $\lambda = 0$. Then, if the vortex is cyclonic, with the potential vorticity inside the vortex exceeding the value outside, we would expect the azimuthal velocity $V(r)$ at the boundary of the vortex to be anticlockwise, i.e. positive. Consequently, $V\mathrm{d}Q/\mathrm{d}r$ will be zero everywhere except at the boundary of the vortex, where it will be negative. Similarly, if the vortex is anticyclonic, with $\mathrm{d}Q/\mathrm{d}r > 0$, we expect $V(r) < 0$ at the vortex boundary. In either case, $V(r)\,\mathrm{d}Q/\mathrm{d}r < 0$ at the vortex boundary, and (2) is not satisfied. Therefore it is not possible to obtain any stability results for an axisymmetric vortex with a monotonic potential vorticity profile by variational methods, no matter how small the Froude and Rossby numbers might be.† This is in stark contrast to the two-dimensional Euler and quasi-geostrophic equations, in which variational methods are sufficient to prove the stability of axisymmetric vortices with a monotonic potential vorticity profile.

An instability of axisymmetric vortices with monotonic potential vorticity was first discovered by Broadbent & Moore (1979), who demonstrated numerically that a Rankine vortex in a compressible fluid is unstable to two-dimensional perturbations for all non-zero Mach numbers, up to the point at which the vortex core evacuates. The Rankine vortex has uniform vorticity, rather than potential vorticity, but the potential vorticity in the vortex can be shown to be monotonic for all Mach numbers. The two-dimensional compressible gas equations are equivalent to the shallow-water equations

† Ripa's theorem is the analogue of Arnol'd's first theorem, in which the second variation is required to be positive for stability. It is straightforward to show that, for the shallow-water system, no analogue of Arnol'd's second theorem can exist, in which the second variation is required to be negative. I thank T. G. Shepherd and T. E. Dowling for discussions on this point.

in the limit of no background rotation, provided the ratio of specific heats $\gamma = 2$. The acoustic waves in the compressible gas equations are the analogues of gravity waves in the shallow-water equations. Although Broadbent & Moore's numerical results took $\gamma = 1.4$, it seems likely that the same instability mechanism would be found with $\gamma = 2$. Additional modes for the Rankine vortex were found by Sozou (1987). However, it is shown in Ford (1993) that these modes owe their existence to the non-uniform potential vorticity in a Rankine vortex at non-zero Mach number, and are therefore excluded from the present study. The contribution of the present paper is to investigate the nature of the instability found by Broadbent & Moore when the Coriolis force is present. The instability found by Broadbent & Moore is also of interest in the stability of accretion discs, studied first by Papaloizou & Pringle (1984, 1985, 1987), and more recently extended to the nonlinear regime by Shukhman (1991) and Williams (1992).

In the remainder of this paper, the instability of an axisymmetric vortex with a single discontinuity in potential vorticity is investigated. In §2, the instability problem is formulated, and the perturbation equations are presented. In §3, the instability is analysed at small Froude number. The present results agree with those of Broadbent & Moore (1979) in the case $f = 0$, since vorticity and potential vorticity are the same in the limit $F \to 0$, and the value of γ is not important to the growth rate of the instability at leading order in F or M. In §4 the growth rates of the instability are obtained numerically. The results at finite Froude number now differ from those of Broadbent & Moore (1979) at finite Mach number, in that in this study the potential vorticity, rather than vorticity, is taken to be constant within the vortex. This prevents the evacuation of the basis state at large F found by Broadbent & Moore. Moreover, the Coriolis force is present, and as the background rotation rate f is increased, the low-mode-number disturbances to the vortex cease to be unstable. In §5, a WKBJ analysis of the instability is performed, and it is found that large-mode-number disturbances to an axisymmetric vortex are always unstable, no matter how small the Froude and Rossby numbers might be. As pointed out by Knessel & Keller (1992) in another context, the WKBJ analysis helps to reveal the mechanism of the instability, as well as establish its existence. A WKBJ analysis for the related problem in accretion discs was undertaken by Papaloizou & Pringle (1987) – the principal difference between their analysis and the present one being that they obtained the growth rate of the instability via an energy argument, whereas in this paper it is obtained explicitly by carrying exponentially small terms in the asymptotic expansions for large mode number. The mechanism of the present instability is discussed in §6, and the relevance of this work to the question of existence or non-existence of a slow manifold for the shallow-water equations in the sense of Leith (1980) is discussed.

2. Formulation of the problem

This paper addresses the instability of axisymmetric vortices in rotating shallow water. The rotating shallow-water equations are

$$\frac{\partial \boldsymbol{u}}{\partial t} + \boldsymbol{u}\cdot\nabla\boldsymbol{u} + f\boldsymbol{k}\times\boldsymbol{u} + g\nabla h = 0, \tag{3}$$

$$\frac{\partial h}{\partial t} + \nabla\cdot(h\boldsymbol{u}) = 0, \tag{4}$$

where $\boldsymbol{u}$ is the two-dimensional velocity field, h is the layer depth, f is the inertial frequency, g is the acceleration due to gravity, and $\boldsymbol{k}$ is a unit vector perpendicular to

the (x, y)-plane. In general, f is a function of position, but in this paper we shall take f to be constant (commonly referred to as the f-plane approximation). The equations are then non-dimensionalized, taking vortex radius as the lengthscale, and (vortex radius)/(azimuthal velocity in vortex) as the timescale. The inertial period, $2\pi/f$, and Rossby deformation radius, $(gh(\infty))^{1/2}f$, are not used to non-dimensionalize the problem, since they are singular in the limit $f = 0$ which was studied by Broadbent & Moore (1979). Since the problem is clearly well defined in the limit $f \to 0$, we do not use a scaling which is singular in that limit. The gravitational acceleration, g, can be absorbed into the height field, and the resulting non-dimensional rotating shallow-water equations are

$$\frac{\partial \boldsymbol{u}}{\partial t} + \boldsymbol{u}\cdot\nabla\boldsymbol{u} + f\boldsymbol{k}\times\boldsymbol{u} + \nabla h = 0, \tag{5}$$

$$F^2\left(\frac{\partial h}{\partial t} + \nabla\cdot(h\boldsymbol{u})\right) + \nabla\cdot\boldsymbol{u} = 0, \tag{6}$$

where now F is the Froude number, f may be regarded as an inverse Rossby number, and F^2h represents the departure of the total layer depth from the mean layer depth, which is unity, so the total layer depth H is given by $H \equiv 1 + F^2h$. The potential vorticity is then given by

$$Q = \frac{f + \boldsymbol{k}\cdot\nabla\times\boldsymbol{u}}{1 + F^2h}. \tag{7}$$

2.1. *The basic state*

Equations for the basic state of an axisymmetric vortex can then be written:

$$\frac{\mathrm{d}\bar{h}}{\mathrm{d}r} = f\bar{v} + \frac{\bar{v}^2}{r}, \tag{8}$$

$$\frac{\mathrm{d}\bar{v}}{\mathrm{d}r} + \frac{\bar{v}}{r} = Q(1 + F^2\bar{h}) - f, \tag{9}$$

where the overbar represents the basic-state value of the field. Equations (8) and (9) must be solved subject to regularity conditions at $r = 0$, and decay conditions as $r \to \infty$. The nonlinearity in (8) means that we must use numerical means to solve (8) and (9), except in the limit $F \ll 1$, where they can be solved by matched asymptotic expansion.

The free parameters in the problem are f and F. The non-dimensionalizations allow us to take the vortex to be of unit radius, and the potential vorticity jump across the boundary of the vortex to be of unit strength. The layer is of unit mean depth. Then $Q = f$ for $r > 1$, and $Q = f + 1$ for $r < 1$.

2.2. *The disturbance equations*

Disturbance equations are derived for a single azimuthal wavenumber m and frequency ω, so that the disturbance variables are expressible in the form $g(r)\,\mathrm{e}^{\mathrm{i}m\theta - \mathrm{i}\omega t}$. The disturbance equations are

$$\mathrm{i}\sigma v_r - (f + 2\bar{v}/r)\,v_\theta + \frac{\mathrm{d}h}{\mathrm{d}r} = 0, \tag{10}$$

$$\mathrm{i}\sigma v_\theta + Q(1 + F^2\bar{h})\,v_r + \frac{1}{r}\mathrm{i}mh = 0, \tag{11}$$

$$F^2(\mathrm{i}\sigma h + (f\bar{v} + \bar{v}^2/r)\,v_r) + (1 + F^2\bar{h})\left(\frac{\mathrm{d}v_r}{\mathrm{d}r} + \frac{v_r}{r} + \frac{1}{r}\mathrm{i}mv_\theta\right) = 0, \tag{12}$$

where $\sigma = -\omega + m\bar{v}/r$, and v_r, v_θ and h are the perturbation radial velocity, azimuthal velocity and height fields respectively. This set of equations must be solved subject to regularity conditions at $r = 0$, and a radiation/evanescence condition as $r \to \infty$.

The equations (10)–(12) contain only two radial derivatives, and therefore represent a second-order differential equation for the eigenfunctions. If one chooses v_r and h as variables, v_θ must be obtained from (11). The possibility of a critical layer at $\sigma = 0$ makes it impossible to ensure, without further analysis, that this will be a successful method. Instead, we choose to eliminate h. After some algebra, one obtains a pair of first-order ordinary differential equations for the eigenfunctions:

$$\frac{\mathrm{d}v_r}{\mathrm{d}r} = A(r)\,v_r + B(r)\,v_\theta, \tag{13}$$

$$\frac{\mathrm{d}v_\theta}{\mathrm{d}r} = C(r)\,v_r + D(r)\,v_\theta, \tag{14}$$

where

$$A(r) = \frac{F^2\sigma Q r}{m} - \frac{1}{r} - \frac{\mathrm{d}}{\mathrm{d}r}\ln H, \tag{15}$$

$$B(r) = \frac{\mathrm{i}F^2\sigma^2 r}{Hm} - \frac{\mathrm{i}m}{r}, \tag{16}$$

$$C(r) = \frac{\mathrm{i}F^2 H Q^2 r}{m} + \frac{\mathrm{i}m}{r} + \frac{\mathrm{i}H}{\sigma}\frac{\mathrm{d}Q}{\mathrm{d}r}, \tag{17}$$

$$D(r) = -\frac{F^2 Q\sigma r}{m} - \frac{1}{r}, \tag{18}$$

and $H = 1 + F^2\bar{h}$.

The advantage of this formulation over the standard formulation (10)–(12) is that the critical-layer singularity $\sigma = 0$ occurs only where there are radial gradients of the basic-state potential vorticity $Q(r)$.† If the potential vorticity gradients are confined to a single discontinuity in potential vorticity at the vortex boundary, then the eigenfunction equations are non-singular, and at the vortex boundary we impose continuity of h and v_r. Dividing (11) by v_r, we thereby obtain a continuity equation

$$\left[\sigma\frac{v_\theta}{v_r}\right] = [\mathrm{i}Q(1 + F^2\bar{h})], \tag{19}$$

where $[\alpha]$ represents the jump in a quantity α across the vortex boundary.

3. The limit $F \ll 1$

Before proceeding to numerical calculation of the eigenvalues of the system (13)–(18), we consider the limit $F \ll 1$. In this limit, an interpretation is possible in terms of the Lighthill theory of aerodynamic sound generation (Lighthill 1952). Perturbations to the boundary of an axisymmetric vortex excite gravity waves on a

† If the equations had been retained in their standard form (10)–(12) and the neighbourhood of $\sigma = 0$ analysed, we would have found that the apparent singularity was actually removable provided $\mathrm{d}Q/\mathrm{d}r$ was zero at $\sigma = 0$. There is no physical difference between the two formulations, but the latter formulation, with no apparent singularity, is better suited to numerical computation.

lengthscale of order F^{-1} longer than the vortex lengthscale. The resulting energy flux implies that the vortex loses energy. Since the axisymmetric vortex is an energy maximum for the two-dimensional incompressible fluid equations, the perturbations to the vortex boundary must grow in response to loss of energy to infinity by acoustic wave radiation. This point of view was first proposed by Kop'ev & Leont'ev (1983). However, in this section we will not appeal to energy arguments, and rely rather on the full details of the matched asymptotic analysis to obtain the growth rates of the instability.

3.1. *The basic state*

We begin our analysis by establishing the form of the basic state from considering the basic-state equations (8) and (9) in the limit $F \ll 1$. From the analyses of Crow (1970) and Ford (1993), we require two asymptotic regions: $r = O(1)$ and $r = O(F^{-1})$.

We begin with the region $r = O(1)$. We expand

$$\bar{v} = \bar{v}_0 + F^2\bar{v}_2 + \ldots, \tag{20}$$

$$\bar{h} = \bar{h}_0 + F^2\bar{h}_2 + \ldots. \tag{21}$$

Here we allow for the possibility that the matching conditions might introduce $\ln F$-terms into the expansions (20) and (21). Substituting (20) and (21) into (9), and imposing regularity at $r = 0$, and r^{-1} decay as $r \to \infty$, we obtain expressions for $\bar{v}$ and $\bar{h}$ at leading order in F:

$$\bar{v}_0 = \begin{cases} \frac{1}{2}r & \text{for} \quad r < 1 \\ \frac{1}{2}r^{-1} & \text{for} \quad r > 1, \end{cases} \qquad \bar{h}_0 = \begin{cases} \frac{1}{8}(2f+1)r^2 + C_1 & \text{for} \quad r < 1 \\ \frac{1}{2}f\ln r - \frac{1}{8}r^{-2} + C_2 & \text{for} \quad r > 1, \end{cases} \tag{22}$$

where C_1 and C_2 are constants, to be determined by continuity of $\bar{h}_0$ at $r = 1$, and matching to the outer solution.

Proceeding now to the outer region, we define a long-range variable $R = Fr$. Since $\bar{v}_0 \sim r^{-1}$ as $r \to \infty$, we rescale $\bar{v}_0$ by F, so

$$\bar{h}_0 = H(R) + O(F^2), \tag{23}$$

$$\bar{v}_0 = FV(R) + O(F^3). \tag{24}$$

Then substituting (23) and (24) into (8) and (9), and imposing decaying boundary conditions as $R \to \infty$ and matching conditions to the solution (22) in the vortical region, $V(R)$ and $H(R)$ are given by

$$V(R) = \tfrac{1}{2}|f|\mathrm{K}_1(|f|R); \quad H(R) = -\tfrac{1}{2}f\mathrm{K}_0(|f|R), \tag{25}$$

where K_0 and K_1 are the modified Bessel functions of order zero and one respectively. For small R, we have

$$H(R) = \tfrac{1}{2}f(\ln(\tfrac{1}{2}|f|R) + \gamma) + O(R^2 \ln R), \tag{26}$$

and matching to (22) gives $\qquad C_2 = \tfrac{1}{2}f(\ln(\tfrac{1}{2}|f|F) + \gamma).$ (27)

Note the appearance of the $\ln F$-term. This means that the expansion for $\bar{h}_0$ starts with a constant term of $O(\ln F)$. Then finally

$$C_1 = \tfrac{1}{2}f(\ln(\tfrac{1}{2}|f|F) + \gamma) - \tfrac{1}{4}(f+1). \tag{28}$$

The analysis presented is valid in the limit $f \to 0$, in which limit

$$V(R) = \frac{1}{2R}; \quad H(R) = O(F^2); \quad C_1 = -\tfrac{1}{4}; \quad C_2 = 0. \tag{29}$$

Having obtained the leading-order solutions for $\bar{v}_0$ and $\bar{h}_0$ in both asymptotic regions, we could now go on to develop perturbation expansions to obtain equations for $\bar{v}_2, \bar{h}_2 \ldots$. However, as we shall see, higher-order terms in the asymptotic expansions for $\bar{v}$ and $\bar{h}$ are not required to compute the growth rate of the instability, and serve only to correct the real part of the eigenfrequency. Indeed, the expression for $\bar{h}_0$ is not essential to the $F \ll 1$ analysis, although it is required to initialize the numerical eigenvalue calculations in the $F \ll 1$ limit.

3.2. *The disturbance equations*

As for the analysis of the basic state, we expand the perturbation radial and azimuthal velocities v_r and v_θ in asymptotic series, with F^2 as the expansion parameter. The asymptotic expansions are matched between two regions, with range variables r and $R \equiv Fr$ as before. Additionally, the eigenvalue ω must be expanded in powers of F^2, with logarithmic terms as necessary.

Substituting (15)–(18) into (13) and (14) in the limit $F \ll 1$ gives equations for v_r and v_θ:

$$\frac{\mathrm{d}v_r}{\mathrm{d}r} = -\frac{1}{r}v_r - \frac{\mathrm{i}m}{r}v_\theta, \tag{30}$$

$$\frac{\mathrm{d}v_\theta}{\mathrm{d}r} = \frac{\mathrm{i}m}{r}v_r - \frac{1}{r}v_\theta. \tag{31}$$

The solutions are $$v_r = r^{m-1}; \quad v_\theta = \mathrm{i}r^{m-1}, \tag{32}$$

or $$v_r = r^{-m-1}; \quad v_\theta = -\mathrm{i}r^{-m-1}. \tag{33}$$

Regularity as $r \to 0$ implies that we take an eigenfunction of form (32) in $r < 1$. Decay as $r \to \infty$ implies that we take an eigenfunction of form (33) in $r > 1$. Then, substituting into the continuity equation (19) gives $\omega = m\bar{v}(1) - \frac{1}{2}$. In the limit $F = 0$, perturbations to the boundary of an axisymmetric vortex with uniform potential vorticity were analysed by Kelvin (1880), who found that the eigenfrequency ω_0 of the disturbances was given by

$$\omega_0 = \tfrac{1}{2}(m-1). \tag{34}$$

The present result is consistent with Kelvin's since, from (22), $\bar{v}(1) = \frac{1}{2} + O(F^2)$, and (34) thus gives the leading-order eigenfrequency for the present problem.

Rather than proceeding to consider higher orders in F in the inner expansion, we will now consider the leading-order outer expansion. There the disturbance equations are

$$\frac{\mathrm{d}v_r}{\mathrm{d}R} = -\left(\frac{\omega_0 f R}{m} + \frac{1}{R}\right)v_r + \left(\frac{\mathrm{i}\omega_0^2 R}{m} - \frac{\mathrm{i}m}{R}\right)v_\theta, \tag{35}$$

$$\frac{\mathrm{d}v_\theta}{\mathrm{d}R} = \left(\frac{\mathrm{i}f^2 R}{m} + \frac{\mathrm{i}m}{R}\right)v_r + \left(\frac{f\omega_0 R}{m} - \frac{1}{R}\right)v_\theta. \tag{36}$$

They have solution

$$v_r = A\left[\mathrm{i}\omega_0 \lambda \mathrm{H}_{m-1}(\lambda R) - \mathrm{i}\frac{m}{R}(\omega_0 + f)\,\mathrm{H}_m(\lambda R)\right], \tag{37}$$

$$v_\theta = A\left[f\lambda \mathrm{H}_{m-1}(\lambda R) - \frac{m}{R}(\omega_0 + f)\,\mathrm{H}_m(\lambda R)\right], \tag{38}$$

where $\lambda^2 = (\omega_0^2 - f^2)$, H_m is a Hankel function of degree m, of the first or second kind,

and A is an arbitrary constant. The kind of the Hankel function is chosen to give radiation conditions at infinity. With $e^{-i\omega t}$ time dependence, one chooses Hankel functions of the first kind for radiation conditions.

Now the outer limit of the leading-order inner expansions for v_r and v_θ must match onto the Hankel functions in the wave region. This implies that, at leading order in F, v_r and v_θ must have r^{-m-1} behaviour in the limit $r \to \infty$. Therefore in the outer region we start our expansions for v_r and v_θ with Hankel functions at $O(F^{m+1})$. If a formal expansion is carried out for the inner region, we see from (15)–(18) that it proceeds by first obtaining the fields at a given order, and then obtaining ω at that order from the continuity condition (19). To obtain v_r and v_θ to order F^{2n} for some integer n, one need only know ω to order $F^{2(n-1)}$. The continuity condition (19) then gives ω at order F^{2n}.

Since the eigenvalue equations are linear in v_r and v_θ, the amplitude of the leading-order solution given by (32) for $r < 1$ and (33) for $r > 1$ is not specified uniquely, and at higher orders in the perturbation expansion it is possible to add to the solution at that order a component of the leading-order eigenfunction. To specify the eigenfunction uniquely, we impose the condition that the coefficients of r^{m-1} in the expansions of v_r and v_θ in the limit $r \to 0$ are zero at all orders in F except the leading order. This then fixes the amplitude and phase of the eigenfunction at all orders in F. Then, without reference to the outer expansion, one can see that the velocity components v_r and v_θ remains $\frac{1}{2}\pi$ out of phase with each other at all subsequent orders in F in the inner expansion, and therefore ω remains real up to the order in F at which the matching conditions with the wave region must be taken into account.

Matching (33) onto (37) and (38) to determine the amplitude of the gravity waves in the outer expansion gives

$$A = -\frac{\pi\lambda^m}{2^m m!(\omega_0+f)}. \tag{39}$$

Then matching the out-of-phase J_m terms in the Hankel functions (37) and (38) back onto the inner solution at $O(F^{2m})$ gives a contribution to the inner solution of the form

$$v_r = -iBr^{m-1}; \quad v_\theta = Br^{m-1}, \tag{40}$$

where B is determined from A and the properties of the Hankel function in the limit $R \to 0$. It is given by

$$B = \frac{\pi m}{(m!)^2}\left(\frac{\omega_0^2 - f^2}{4}\right)^m \left(\frac{\omega_0 - f}{\omega_0 + f}\right). \tag{41}$$

As discussed above, to make the expansion procedure well defined, the expansions for v_r and v_θ in $r < 1$ are to be $o(r^{m-1})$ for $r \ll 1$, and hence we must add to (40) functions of form (33) to ensure continuity of v_r at $r = 1$. All other contributions to v_r and v_θ at all orders up to and including F^{2m} contribute only to the real part of ω, and not to the growth of the instability.

To calculate the growth rate of the instability, it is therefore sufficient to consider the velocity fields

$$v_r = \begin{cases} r^{m-1} & \text{for} \quad r > 1 \\ r^{-m-1} - iBF^{2m}(r^{m-1} - r^{-m-1}) & \text{for} \quad r < 1, \end{cases} \tag{42}$$

$$v_\theta = \begin{cases} ir^{m-1} & \text{for} \quad r < 1 \\ -ir^{-m-1} + BF^{2m}(r^{m-1} + r^{-m-1}) & \text{for} \quad r > 1. \end{cases} \tag{43}$$

Returning to the jump condition (19), we obtain

$$\mathrm{Im}(\omega) = \frac{\pi m F^{2m}}{2(m!)^2}\left(\frac{\omega_0^2 - f^2}{4}\right)^m \left(\frac{\omega_0 - f}{\omega_0 + f}\right) + O(F^{2m+2}), \tag{44}$$

which is consistent with the results of Kop'ev & Leont'ev (1983) in the case $f = 0$.

4. Numerical eigenvalue calculations

We now turn to investigating the growth rates of the instability at values of F which are not sufficiently small that the growth rate can be obtained by asymptotic analysis at small F. To do this, we employ numerical means to solve for the basic state and the eigenfunctions and eigenvalues, as F is gradually increased, for various values of the azimuthal mode number m.

4.1. *Numerical technique*

We start by considering techniques for solving numerically the basic equations (8) and (9) for the basic-state variables $\bar{v}$ and $\bar{h}$. The numerical difficulties arise in that both $r = 0$ and $r = \infty$ are singular points of the system, and we can only apply boundary conditions there by making use of some expansion of the solutions for small r and large r respectively. Given initial guesses for $\bar{h}(0)$ and $\bar{h}(\infty)$, the basic-state equations can then be integrated to $r = 1$, and iteration on $\bar{h}(0)$ and $\bar{h}(\infty)$ using Newton's method is employed to make $\bar{h}$ and $\bar{v}$ continuous across the vortex boundary $r = 1$. In $r > 1$, the solution is exponentially decaying at large r, and so the far-field form of the solution is factored out from the numerical integration, so that the numerically computed variables remain of order unity throughout the range of integration. The details of the implementation of the numerical algorithm for obtaining the basic states are given in Appendix A.

We now turn to the disturbance equations. The analysis of the eigenvalue equations is simplified by noting that the amplitude of the eigenfunctions is irrelevant, and that from (19) only the ratio v_r/v_θ on either side of the vortex boundary is required to compute the eigenvalue ω. As for the basic state, both $r = 0$ and $r = \infty$ are singular points of the equations, and some use must be made of the asymptotic form of the solution in these limits to apply the appropriate boundary conditions, which are boundedness at $r = 0$ and evanescence as $r \to \infty$. Again, as in the case of the basic state, the equations for the disturbances are integrated from $r = 0$ and $r = \infty$ using starting series, and ω is then iterated to satisfy the matching condition (19) at $r = 1$. The details of the implementation of the numerical algorithm for obtaining the eigenvalues are given in Appendix B.

4.2. *The basic state*

Before discussing the nature of the instability found for vortices with a single radial discontinuity in potential vorticity, it is instructive to examine the way in which the basic states themselves depend on the parameters of the problem: F and f.

In figure 1, the basic-state velocity and height profiles are shown, as a function of radius, for $F = 0.2$, and for three families of vortex:

(i) cyclones, with potential vorticity in the vortex of the same sign as the background value – velocity and height profiles are shown for $f = 0.1$, 0.2, 0.3, 0.4 and 0.5;

(ii) anticyclones with potential vorticity in the vortex of the opposite sign to the background value – velocity and height profiles are shown for $f = -0.1$, -0.3, -0.5, -0.7 and -0.9;

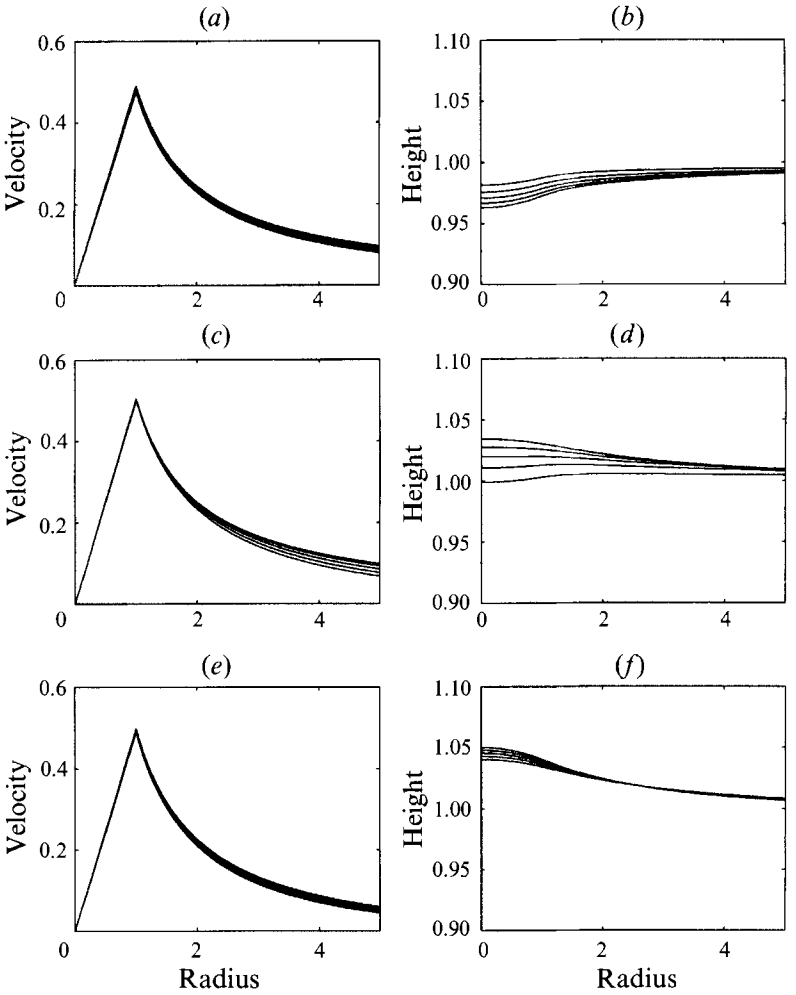

FIGURE 1. Basic-state velocity and height fields: $F = 0.2$. (*a*) Velocity for $f = 0.1$, 0.2, 0.3, 0.4 and 0.5. The velocity decays more rapidly with r as f is increased. (*b*) The corresponding height field as a function of r. The depression at $r = 0$ increases as f is increased. (*c*, *d*) As (*a*, *b*) but with $f = -0.1$, -0.3, -0.5, -0.7 and -0.9. The velocity decays more rapidly with increasing $|f|$, and the surface elevation at $r = 0$ increases with increasing $|f|$. (*e*, *f*) As (*a*, *b*), but with $f = -1.1$, -1.2, -1.3, -1.4 and -1.5. Again, velocity decays more rapidly with r as $|f|$ is increased, and the surface elevation at $r = 0$ increases as $|f|$ is increased.

(iii) anticyclones with potential vorticity in the vortex of the same sign as the background value – velocity and height profiles are shown for $f = -1.1$, -1.2, -1.3, -1.4 and -1.5.

The velocity and height profiles in all cases are much as expected from the analysis for $F \ll 1$. Within the vortex (i.e. $r < 1$) the velocity increases almost linearly with r, reaching a maximum value of approximately 0.5 at $r = 1$. Outside the vortex the velocity decays with r, at first almost as r^{-1}, and eventually decays more rapidly with r at larger r. Cases with larger values of $|f|$ exhibit more rapid decay with r than those with smaller values of $|f|$. In the height field, cyclones correspond to depressions of the height field (figure 1*b*), whereas anticyclones with potential vorticity of the same sign as the background correspond to elevations (figure 1*f*). A transition between the two

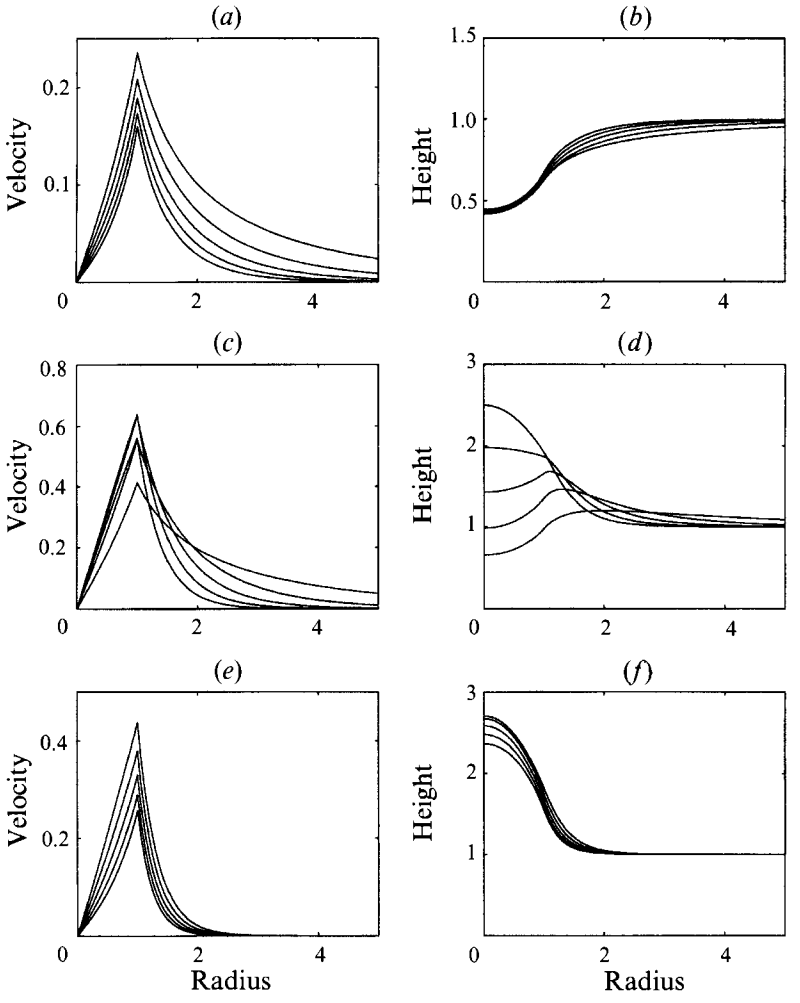

FIGURE 2. Basic-state velocity and height fields: $F = 2.5$. Other details as in figure 1, except that in this case the surface elevation decreases with increasing $|f|$ in (f).

limits is observed in the case of anticyclones with potential vorticity of opposite sign to the background value (figure 1d).

In figure 2, the basic-state velocity and height fields are shown for the same values of f as in figure 1, but now with the Froude number $F = 2.5$. The cyclones now correspond to much more severe depressions of the free surface than was the case at $F = 0.2$, and the velocity within the vortex has decreased relative to its value at $F = 0.2$. In the case of anticyclones with potential vorticity of opposite sign to the background, the velocity at the boundary of the vortex has not been reduced significantly from its value at $F = 0.2$, and in some cases has risen above that value. The transition between depression and elevation as f is varied from -0.1 to -0.9 is now clearly seen in figure 2(d). Finally, in the case of anticyclones with potential vorticity of the same sign as the background, the velocity at the boundary of the vortex is seen to have decreased relative to its value at $F = 0.2$, with the effect becoming more pronounced at larger values of $|f|$.

Finally, in figure 3, the basic-state velocity and height fields are shown for $F = 5.0$.

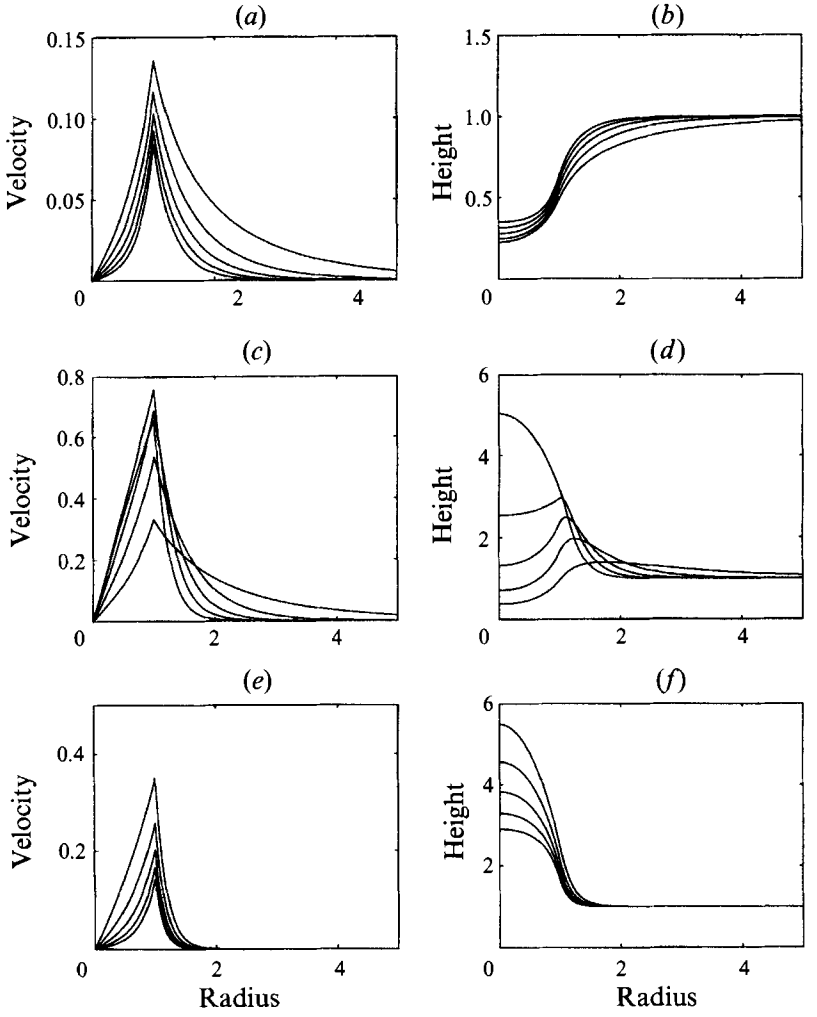

FIGURE 3. Basic-state velocity and height fields: $F = 5.0$. Other details as in figure 2.

They serve to reinforce the trends observed from $F = 0.2$ to $F = 2.5$. In particular, in the case of cyclones, the layer depth at the centre of the vortex is now only about one-quarter of its value far from the vortex, whereas in the case of anticyclones with potential vorticity of the same sign as the background, the layer depth at the centre of the vortex can exceed five times the layer depth far from the vortex.

4.3. *Results of the eigenvalue calculations*

The growth rate of the instability of the axisymmetric vortex depends on three parameters: the Froude number F; the Rossby number f^{-1}; and the azimuthal mode number of the instability m.

We begin by investigating the growth rates of the instability in the case of infinite Rossby number ($f = 0$). This limit is most similar to the study of Broadbent & Moore (1979), except here we take the vortex to have uniform potential vorticity, rather than uniform vorticity as they did.

Figure 4(*a*) shows the growth rates of the instability for Froude numbers from 0 to

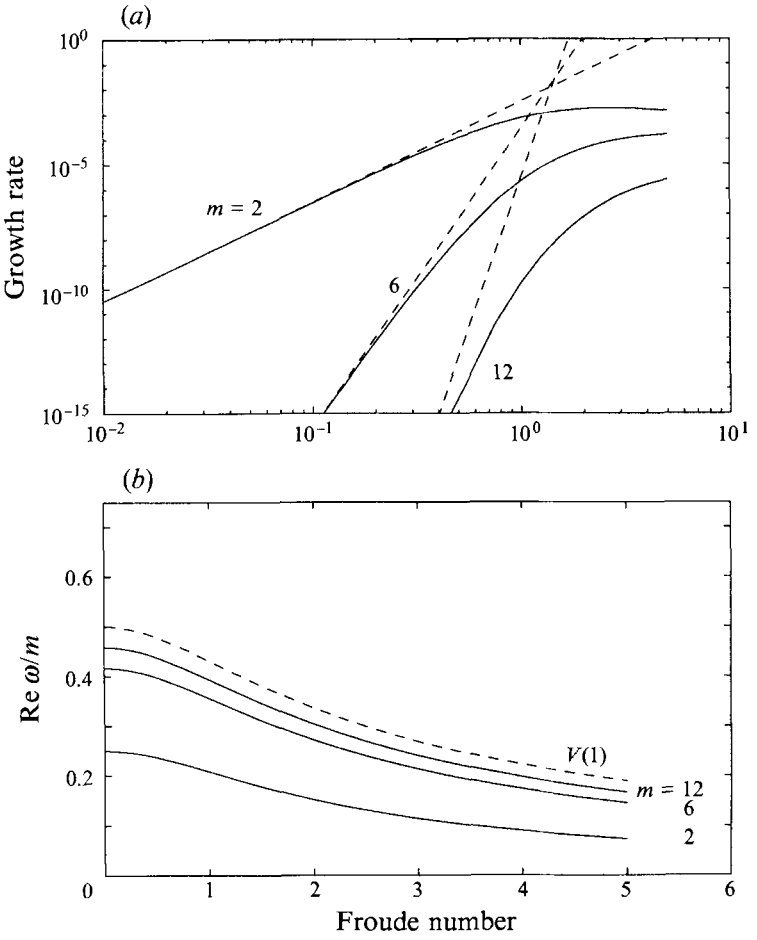

FIGURE 4. Axisymmetric vortex with $f = 0$. (*a*) Growth rates of the instability (solid lines) with growth rates predicted in the small-Froude-number limit (dashed lines). (*b*) Real parts of the eigenfrequencies $\mathrm{Re}\,\omega/m$ (solid lines) and $V(1)$ (dashed line).

5 and for mode numbers $m = 2$, 6, 12. Solid lines are growth rates obtained from the numerical eigenvalue calculation, and dotted lines are the growth rates given by the low-Froude-number analysis (equation (44)). The graph is plotted on a log-log scale, so that at low Froude number the slope of the lines is $2m$. Mode 2 is found to be the most unstable, and its growth rate increases more slowly with Froude number than the growth rates at higher mode numbers. The numerical eigenvalue calculations are apparently reproducing the eigenvalues obtained from the low-Froude-number limit with growth rates down to 10^{-14}, and we can be confident that numerical algorithm used to integrate (13) and (14) is performing adequately with the tolerances prescribed. The real part of the eigenfrequency is shown in figure 4(*b*). It is always bounded between 0 and $m \times V(1)$, apparently approaching $m \times V(1)$ at large m.

We now turn to investigating the instability at non-zero f. In particular, it is important to note that for f between 0 and -1 the vortices are anticyclones with potential vorticity of opposite sign to the background potential vorticity. For $f > 0$ the vortices are always cyclones, and for $f < -1$ they are anticyclones with potential vorticity of the same sign as the background. In all cases with $f \neq 0$, we expect the effect

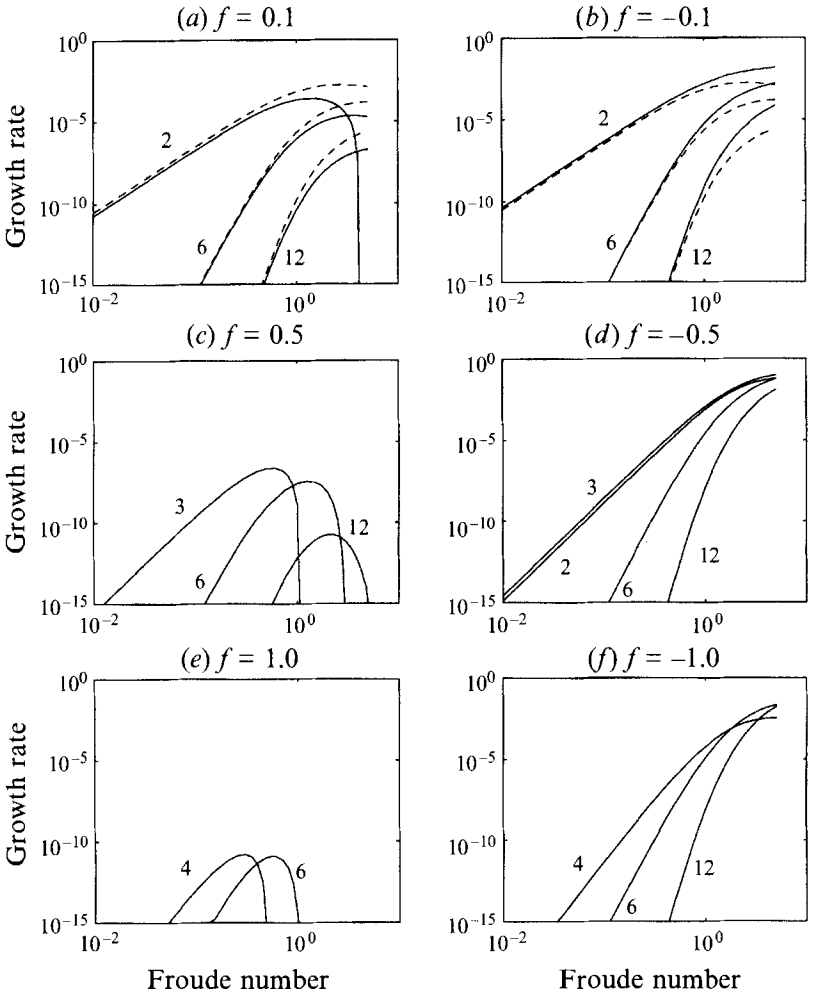

FIGURE 5. Growth rates of instability for axisymmetric vortex with $f = \pm 0.1, \pm 0.5, \pm 1.0$. Labels on curves correspond to values of m. In (*a*) and (*b*) dashed lines correspond to the case $f = 0$.

of background rotation to inhibit the instability if the real part of the eigenfrequency is below $|f|$. We therefore start by investigating the effect on the instability of background rotation with values of $|f| = 0.1$, 0.5 and 1.0.

In figure 5, the growth rates of the instability are shown in each case. Figures 5(*a*) and 5(*b*) correspond to the cases $f = 0.1$ and $f = -0.1$ respectively. At small Froude number, the growth rates are similar to those with $f = 0$. However, as F is increased, the instability at small mode numbers becomes inhibited for $f = 0.1$, but not for $f = -0.1$. Figures 5(*c*) and 5(*d*) show the growth rates of the instability for $f = 0.5$ and $f = -0.5$ respectively. The case $|f| = 0.5$ is significant because, at small Froude numbers, the mode $m = 2$ is marginally stable – i.e. it is unstable for $|f| < 0.5$, and stable for $|f| > 0.5$. In the case $f = 0.5$, mode $m = 2$ turns out to be stable for all F, whereas for $f = -0.5$ mode $m = 2$ becomes unstable for non-zero F, but with the growth rate of the instability increasing as the sixth power of Froude number, at small Froude number, rather than the fourth power. The inhibition of the instability at large Froude numbers in the case of positive f is now more pronounced than for $f = 0.1$, with modes up to $m = 12$ being stable for $F = 5.0$. Finally, figures 5(*e*) and 5(*f*) correspond to

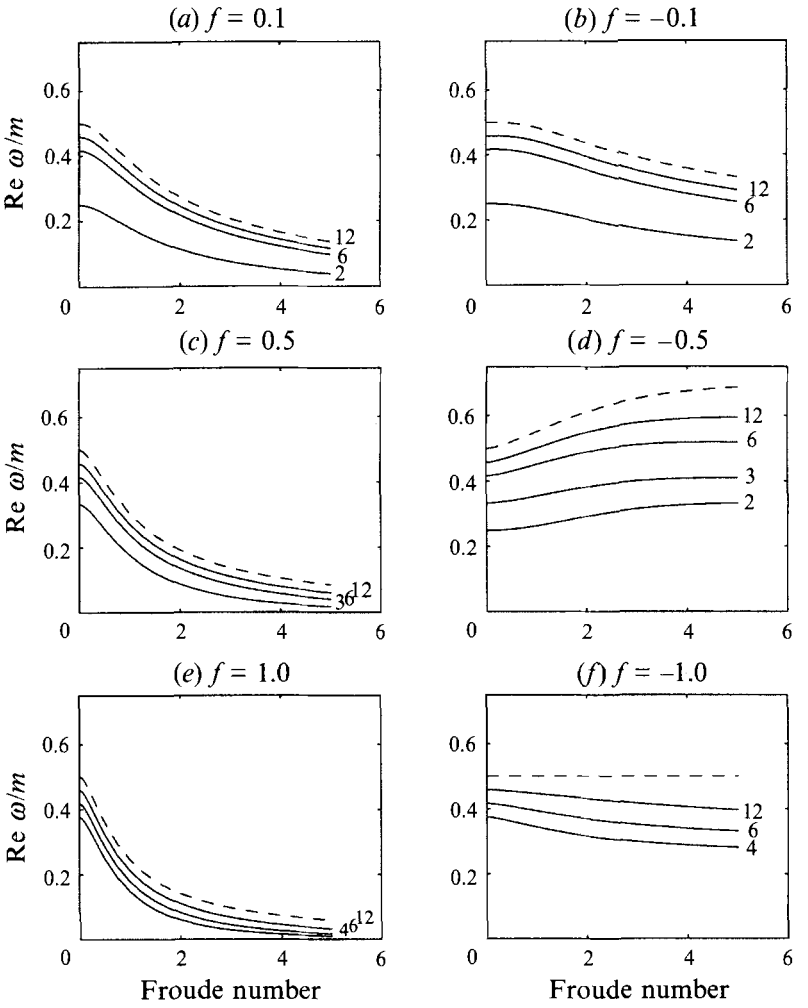

FIGURE 6. Real parts of the eigenfrequency for axisymmetric vortex with $f = \pm 0.1$, ± 0.5, ± 1.0. Labels on curves correspond to values of m. Dashed lines correspond to $V(1)$, the azimuthal velocity at the boundary of the vortex.

$f = 1.0$ and $f = -1.0$. With $|f| = 1.0$, mode $m = 4$ is now marginally stable, and in both cases it remains stable for all Froude numbers. However, the growth rates of the other modes remain markedly different in the two cases, with the maximum growth rate for $f = 1.0$ over all Froude numbers being of order 10^{-11}, whereas for $f = -1.0$ growth rates of order 10^{-2} are observed for large F. The main conclusion to be drawn from figure 5 is that the magnitude of f is not the principal factor in determining the growth rate of the instability.

The real part of the eigenfrequency, divided by the mode number m, is shown in figure 6 for each of the cases shown in figure 5. In general, vortices with $f > 0$ experience a very rapid decrease in ω/m as F is increased, whereas those with $0 > f \geqslant -1$ experience only a moderate decrease in ω/m or, in the case $f = -0.5$, an increase in ω/m. This means that the effect of the inertial cut-off frequency will be felt more strongly when $f > 0$, as ω falls below f, and the eigenmode is no longer unstable as F is increased.

For $f \sim 1$ it appears that the cyclones have instabilities with only very weak growth

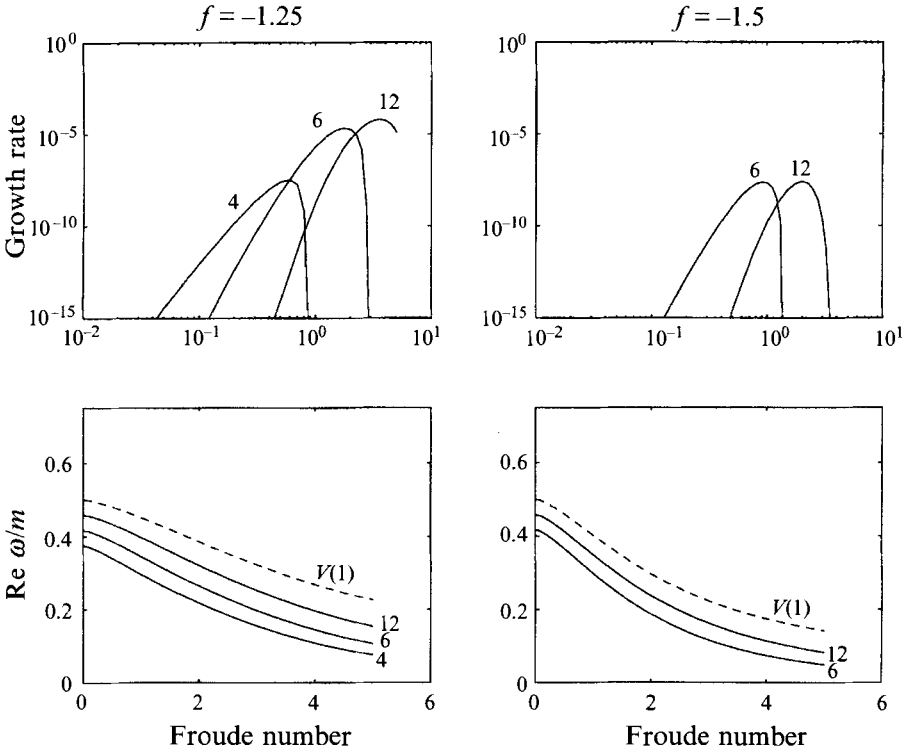

FIGURE 7. Growth rates and real parts of eigenfrequency for $f = -1.25$ and -1.5.

rates, if at all, and it seems likely that increasing f still further will continue to reduce the growth rates, at the same time requiring larger and larger m for the instability to exist at all. However, for $f \sim -1$, the anticyclones still have comparatively large growth rates. To investigate the regime $f < -1.0$, figure 7 shows the growth rates of the instability, and the real part of the eigenvalue, for $f = -1.25$ and $f = -1.5$, and for mode number $m = 4$, 6 and 12. In these cases, the instability at moderate mode numbers m becomes inhibited at larger Froude numbers, and has much in common with the cases of $f > 0$. Similarly, the real parts of the eigenfrequency, and the vortex boundary velocity, decrease significantly as F is increased.

The instability is summarized for all f and F in figure 8. In figure 8(a) the maximum growth rate of the instability taken over all mode numbers m is shown as a function of F and f. One can see that the maximum growth rate of the instability appears to grow without bound for increasing Froude number only in the range $0 \geqslant f \geqslant -1.0$. This is the range in which the potential vorticity in the vortex is of the opposite sign to the background potential vorticity. Outside this range, when the potential vorticity within the vortex is of the same sign as the background potential vorticity, the instability is inhibited at low mode numbers, which otherwise tend to have the largest growth rates, and the maximum growth rate of the instability over all F is quite small – less than 10^{-7} for $f = 0.5$ and -1.5. The mode number m of the fastest growing mode is shown in figure 8(b), confirming that the mode number of the fastest growing mode becomes quite large as F is increased for f outside the range [0, -1.0]. Indeed, with $f = -1.5$ and $F = 5$, the mode number of the fastest growing mode is 27.

We turn now to an explanation of the difference in behaviour of the instability between cyclonic and anticyclonic vortices. At low Froude number, a difference

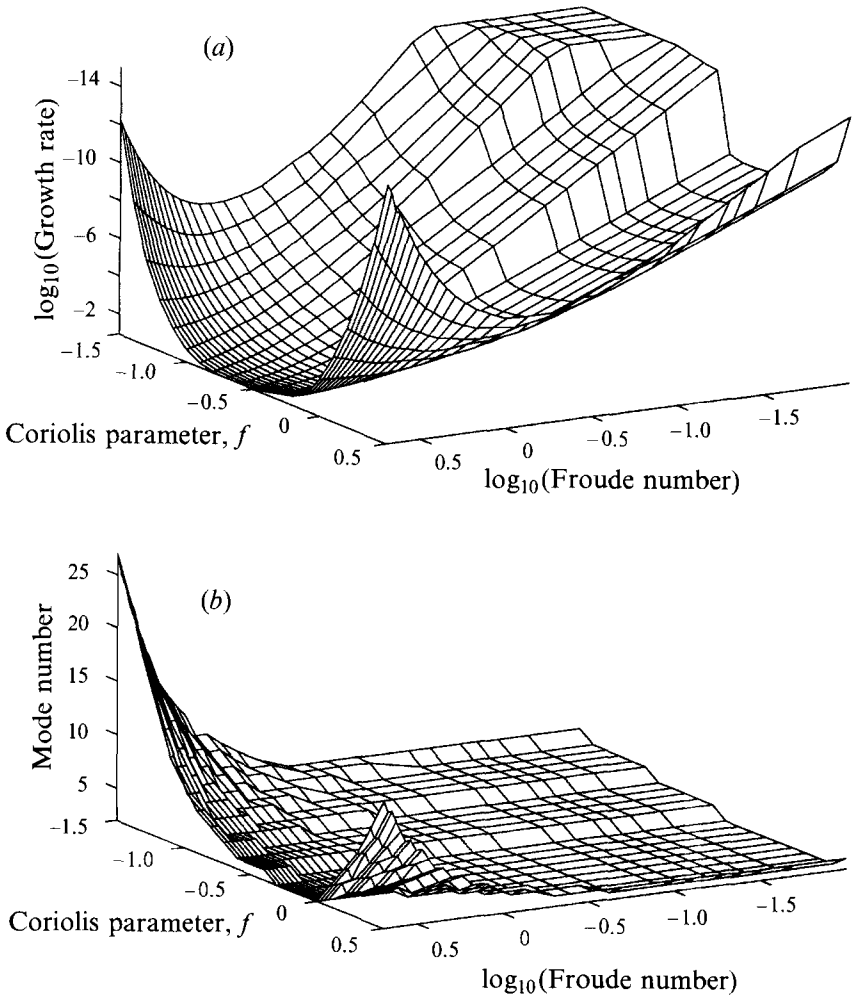

FIGURE 8. Summary of fastest growing mode of axisymmetric vortex instability, for $-1.5 \leqslant f \leqslant 0.5$ and $0 < F < 5$. The flat region for small F and negative f corresponds to growth rates below 10^{-15}. Note the orientation of the growth rate axis: for ease of visualization of the growth rate surface, the figure is shown with the largest growth rates at the bottom, and smallest growth rates at the top. (*a*) Growth rate on $\log_{10} - \log_{10}$ scale. (*b*) Fastest growing mode.

between positive and negative f exists in expression (44) for the growth rate of the instability in the $F \ll 1$ limit. The difference is a factor of $(\omega - f)/(\omega + f)$, which is smaller if ω and f have the same sign than it is if they are of opposite sign. Since ω is always positive, this factor means that anticyclones are always more unstable to this type of instability than cyclones. The difference lies in the nature of the coupling between the vortical region and the wave region. This difference is small, however, and amounts only to a constant factor. It cannot explain why low-wavenumber disturbances to cyclonic vortices are stabilized as the Froude number is increased, whereas low-wavenumber disturbances to anticyclonic vortices are destabilized.

The key to understanding the difference lies in the nature of the basic states. For small F, the azimuthal velocity at the vortex boundary is always 0.5. Since the wave on the boundary of the vortex is a Rossby wave, we expect it to propagate in a pseudo-westward direction – i.e. with a real frequency between 0 and $m \times V(1)$ in the case of

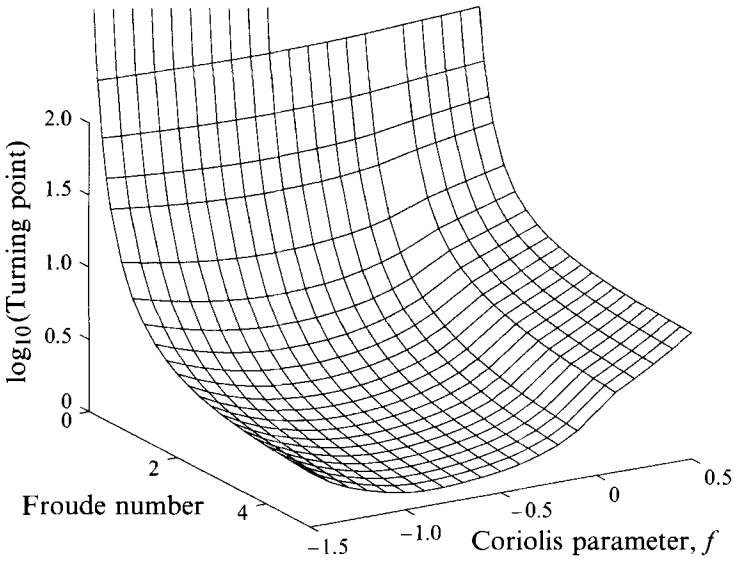

FIGURE 9. Location of turning point for all $0 < F < 5$ and $-1.5 < f < 0.5$.

a vortex of unit radius. Therefore the azimuthal velocity at the boundary of the vortex sets a bound for the real part of the eigenfrequency.

One explanation for the fact that, for a given mode number, eigenmodes with comparatively high frequencies will be more unstable is that they are less influenced by the inertial cut-off $\omega = |f|$. While this is one explanation, it is not the only one, and is probably not the most significant. Regardless of the inertial cut-off frequency, we would still expect higher-frequency eigenmodes to be more unstable than lower-frequency modes, because at higher frequencies the interaction between vortical and gravitational motions becomes stronger.

To see this, first recall that we expect the growth rate of the instability to depend on the strength of coupling between the Rossby wave, on the vortex boundary, and the gravity waves, found distant from the vortex boundary. The character of the eigenmodes changes from being Rossby-wave-like to gravity-wave-like for r of the order of the 'sonic radius', at which the intrinsic angular phase speed of disturbances, $\omega r/m - V(r)$, is equal to the gravity wave phase speed $F^{-1}H^{1/2}(r)$. At a given F and m, it follows that, the larger the value of ω, the smaller r will have to be to achieve a given angular phase speed, and hence the closer the sonic radius will be to the boundary of the vortex. We should expect this to lead to an enhanced coupling between the Rossby wave on the vortex boundary and the gravity wave beyond the sonic radius in cases where ω is comparatively large.

Taking $\omega = m \times V(1)$ – an approximation which is valid to leading order in m for large m – the position of the sonic radius as a function of F and f is shown in figure 9. At small F, the position of the sonic radius is independent of f, and can be shown to be at $r = 2F^{-1}$. However, at larger F, figure 9 shows clearly that the turning point moves closest to the boundary of the vortex in the cases $-1 < f < 0$ – precisely the cases in which the strongest instability is observed.

The results of the eigenvalue calculations may be summarized as follows. In the absence of background rotation, the eigenmode with $m = 2$ is always unstable in the range $0 < F < 5$, and is probably unstable for all F. With background rotation present, low-mode-number eigenmodes may be unstable at small Froude numbers, but become

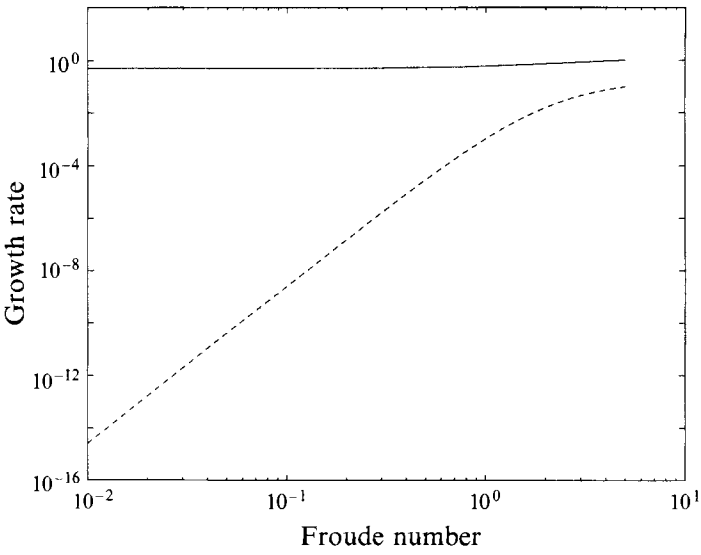

FIGURE 10. Maximum growth rate of inertial instability for $f = -0.5$ (solid line), compared with growth rate for mode number $m = 3$ (dashed line).

stabilized as the Froude number is increased. This is because the real part of the eigenfrequency decreases as the Froude number is increased, and eventually falls below $|f|$, at which point the instability mechanism no longer exists.

From a practical point of view, we have almost certainly identified those cases in which this instability is sufficiently vigorous that it might be observed in nature, and these all occur when f is between -1.0 and 0. Thus, strong instabilities are observed only in cases where the potential vorticity in the vortex is of the opposite sign to the background potential vorticity. However, in a three-dimensional fluid, it can be shown that vortices with potential vorticity of the opposite sign to the background will be inertially unstable, using a modification of Ooyama's (1966) analysis for the f-plane (see Appendix C), and so the instability presented in this paper will be of interest in those cases only if it turns out to be stronger than the inertial instability. To investigate the relative strengths of the two instabilities, the maximum growth rates of inertial instability were obtained for $f = -0.5$, and shown in figure 10, together with the growth rate of the fastest growing mode ($m = 3$) of the present instability. It can be seen from figure 10 that the inertial instability is always stronger than the present instability over the range $0 < F < 5$ in the case $f = -0.5$. The present instability is therefore likely to be significant only near $f = 0$ and $f = -1.0$, which are the boundaries in parameter space for the existence of inertial instability. However, at $f = -1.0$ the e-folding time of the instability is approximately 50 vortex rotation times, and at $f = 0$ is it more than 100 vortex rotation times, and so the present instability is too weak to be of practical significance at the boundaries of the region of inertial instability. Thus it seems that inertial instability is always likely to be the more vigorous instability in the regions of parameter space where the e-folding time of the present instability is small enough that it could have been observed in nature.

However, we are interested not only in cases of practical significance, but also in whether coupling between vortical motions and gravity waves exists at all Rossby numbers, or whether there is a value of $|f|$ above which the instability ceases to exist, at least for some range of F, and in which cases the vortical motions could then be separated from the gravity waves in the problem, in a sense to be made more precise

in §6. The next section, §5, therefore examines this instability for arbitrary f and F in the limit $m \gg 1$. The WKBJ analysis has the added advantage that it assumes *a priori* that $\omega \gg f$. Therefore any distinction between cyclones and anticyclones which can be accounted for by the WKBJ analysis must be due to the general nature of the basic state, and the strength of Rossby wave–gravity wave interactions on it, and any distinction not accounted for by the WKBJ analysis may be regarded as due to the specific effects of the inertial cut-off frequency.

5. The limit of large mode number

We start by writing (13) and (14) as a single second-order ordinary differential equation for v_θ:

$$\frac{\mathrm{d}^2 v_\theta}{\mathrm{d}r^2} + P(r)\frac{\mathrm{d}v_\theta}{\mathrm{d}r} + Q(r)\, v_\theta = 0, \tag{45}$$

where

$$P = -\frac{C'}{C} - A - D; \quad Q = \frac{C'D}{C} + AD - BC - D', \tag{46}$$

where here A, B, C and D are given by (15)–(18). Equation (45) must be solved subject to certain boundary conditions. These are regularity at $r = 0$, and an evanescence/radiation condition as $r \to \infty$. The second condition requires some care. Any unstable mode must be exponentially weak at infinity, and therefore an evanescence condition should suffice. However, we shall for convenience state the radiation condition, bearing in mind that when the eigenfrequency becomes slightly complex, perhaps at some high order in the expansion parameter m, the solution of (45) acquires some weak exponential decay.

Following standard WKBJ analysis, we write

$$v_\theta = \mathscr{A}(r)\, \mathrm{e}^{\mathrm{i}m\psi(r)}, \tag{47}$$

where now $\mathscr{A}(r)$ is an amplitude function and $\psi(r)$ is a phase function, made rapidly varying through the factor m in the exponent. Substituting (47) into (45) gives

$$\mathscr{A}'' + 2\mathrm{i}m\psi'\mathscr{A}' + \mathrm{i}m\psi''\mathscr{A} - m^2\psi'^2\mathscr{A} + P(r)(\mathscr{A}' + \mathrm{i}m\psi'\mathscr{A}) + Q(r)\,\mathscr{A} = 0. \tag{48}$$

In general ψ and $\mathscr{A}$ must be expanded in inverse powers of the WKBJ expansion parameter m. The decomposition of v_θ into $\mathscr{A}(r)$ and $\psi(r)$ is not unique. A small ($O(m^{-1})$, say), correction to v_θ through ψ could just as easily be made by an $O(m^{-1})$ correction to $\mathscr{A}$. However, the decomposition can be made unique, and a great deal more convenient to work with, if we insist that $\mathscr{A}(r)$ and $\psi(r)$ naturally take the roles of amplitude and phase in that, if $\{\mathscr{A}(r), \psi(r)\}$ is a solution of (48), then so is $\{\mathscr{A}(r), -\psi(r)\}$.

Equation (48) can then be separated into two equations:

$$\mathscr{A}'' - m^2\psi'^2\mathscr{A}' + P(r)\,\mathscr{A} + Q(r)\,\mathscr{A} = 0, \tag{49}$$

$$2\psi'\mathscr{A}' + \psi''\mathscr{A} + \psi'\mathscr{A}P(r) = 0, \tag{50}$$

and (50) can be integrated at once to

$$2\ln|\mathscr{A}| + \ln|\psi'| + \int P = 0. \tag{51}$$

We now start our asymptotic analysis of (49). Since we know from (34) that ω is of order m, at least in the limit $F \ll 1$, it is convenient to work with an intrinsic angular

frequency c defined by $c \equiv \omega/m$. Bearing Kelvin's expression $\omega = (m-1)/2$ in mind, and in the spirit of asymptotic expansions, we must extend c in the form

$$c = c_0 + m^{-1}c_1 + \ldots. \tag{52}$$

In fact, it will turn out that c has not only an algebraic expansion in m^{-1}, but also requires terms exponentially small in m to describe the instability.

From (15)–(18) we know that, expanding in m, $P(r)$ is $O(1)$, while $Q(r)$ takes the form

$$Q(r) = m^2\left[\frac{(-c+\bar{v}/r)^2F^2}{1+F^2\bar{h}} - \frac{1}{r^2}\right] + O(1), \tag{53}$$

which can, by virtue of the expansion (52) have terms of $O(m^2)$ and $O(m)$. From (49), at $O(m^2)$, the equation for ψ_0 is

$$\psi_0'^2 = \frac{(-c_0+\bar{v}/r)^2F^2}{1+F^2\bar{h}} - \frac{1}{r^2}. \tag{54}$$

The expression for $\mathscr{A}_0$ can be obtained from (51). Notice that, since $P(r)$ is regular for all $r \neq 0$, there is a singularity in the expression for $\mathscr{A}_0$ at a radius $r = r_c$ where $\psi_0'(r_c) = 0$. We can see at once that, for $c_0 \neq 0$, there is at least one such radius, since $\psi_0'^2 \sim -r^{-2} < 0$ as $r \to 0$, but $\psi_0'^2 \sim c_0^2F^2 > 0$ as $r \to \infty$.

Now, $v_\theta = \mathscr{A}(r)\,e^{im(\psi_0+m^{-1}\psi_1+\ldots)}$, and since we will require an expression for both the amplitude and phase of v_θ, we must obtain expressions for both ψ_0 and ψ_1. The equation for ψ_1 is obtained from (49) at $O(m)$:

$$\psi_0'\psi_1' + \frac{F^2c_1(-c_0+\bar{v}/r)}{1+F^2\bar{h}} = 0. \tag{55}$$

Now, the nature of the solutions for v_θ differs significantly on either side of $r = r_c$. On one side, and in particular in the limit $r \to \infty$, the solutions are oscillatory (for real c_0), whereas on the other side, and in particular in the limit $r \to 0$, they are growing and decaying exponentials. We refer to the radius $r = r_c$ as the 'turning radius', and in the following analysis we shall assume that there is precisely one turning radius for the vortex. There is always precisely one turning radius for $F \ll 1$, whatever the magnitude of the Coriolis parameter f, and hence the assumption includes the basic state in the 'quasi-geostrophic' limit, in which one might expect interactions between vortices and gravity waves to be weakest. All vortices investigated numerically in the previous section were found to have precisely one turning radius.

The expansion (47) for v_θ is not valid in the neighbourhood of $r = r_c$, since ψ_0' is zero there, and so by (51) $\mathscr{A}$ would be unbounded. We must therefore rescale the equations in the neighbourhood of $r = r_c$ and derive equations for the perturbation expansion in this inner asymptotic region. In the vicinity of $r = r_c$, we have

$$Q(r) = m^2a_1(r-r_c) + \ldots, \tag{56}$$

where a_1 is a positive constant. Rescaling the radial coordinate as $x = m^{2/3}(r-r_c)$ the leading-order equation for v_θ from (45) becomes

$$\frac{d^2v_\theta}{dx^2} + a_1xv_\theta = 0. \tag{57}$$

Equation (57) has solutions $v_\theta = \mathrm{Ai}(-a_1^{1/3}x)$, $\mathrm{Bi}(-a_1^{1/3}x)$, where $\mathrm{Ai}(z)$ and $\mathrm{Bi}(z)$ are Airy functions (Abramowitz & Stegun 1965).

Four asymptotic regions have now been established, and the method of matched asymptotic expansions will now be used to relate the solutions in the different regions. The asymptotic regions are: 1, $r > r_c$; 2, $r - r_c = O(m^{-2/3})$; 3, $1 < r < r_c$; 4, $0 < r < 1$.

5.1. *Region* 1: $r > r_c$

As $r \to \infty$, we can place conditions on the branch of square root to take in the solution of (54) by imposing a radiation boundary condition, so that $\psi_0' > 0$ as $r \to \infty$. This immediately implies, through the matching condition in the limit $x \to \infty$, the ratio of Ai to Bi to take in the solution of (57). The expansions of Ai(z) and Bi(z) in the limit $z \to \infty$ then give, through the matching conditions, the ratio of the growing to decaying exponential solutions to (45) for $1 < r < r_c$.

5.2. *Region* 2: $r - r_c = O(m^{-2/3})$

For $z \to -\infty$, the Airy functions take the asymptotic forms

$$\mathrm{Ai}(-z) \sim \pi^{-1/2} z^{-1/4} \sin(\tfrac{2}{3}z^{3/2} + \tfrac{1}{4}\pi), \tag{58}$$

$$\mathrm{Bi}(-z) \sim \pi^{-1/2} z^{-1/4} \cos(\tfrac{2}{3}z^{3/2} + \tfrac{1}{4}\pi). \tag{59}$$

Therefore, if we write $v_\theta = \alpha \mathrm{Ai}(-a_1^{1/3}x) + \beta \mathrm{Bi}(-a_1^{1/3}x)$, matching to a radiating field as $x \to \infty$ implies $\alpha/\beta = \mathrm{i}$.

In the limit $x \to -\infty$ we have

$$\mathrm{Ai}(z) \sim \tfrac{1}{2}\pi^{-1/2} z^{-1/4} \mathrm{e}^{-(2/3)z^{3/2}}, \tag{60}$$

$$\mathrm{Bi}(z) \sim \pi^{-1/2} z^{-1/4} \mathrm{e}^{(2/3)z^{3/2}}. \tag{61}$$

5.3. *Region* 3: $1 < r < r_c$

Now if we let

$$\Psi_0(r) = -\int_r^{r_c} \left(\frac{1}{r^2} - \frac{(-c_0 + \bar{v}/r)^2 F^2}{1 + F^2 \bar{h}} \right)^{1/2} \mathrm{d}r \tag{62}$$

and

$$\Psi_1(r) = \int_r^{r_c} \frac{c_1(-c_0 + \bar{v}/r)}{\Psi_0'(1 + F^2\bar{h})} \mathrm{d}r \tag{63}$$

then, for $1 < r < r_c$, we have

$$v_\theta = A(r)(a\,\mathrm{e}^{m\Psi_0 + \Psi_1} + b\,\mathrm{e}^{-m\Psi_0 - \Psi_1}), \tag{64}$$

where the ratio of b to a is to be determined by the matching conditions to the Airy function region. Now the Bi($-a_1^{1/3}x$)-term is, by (61), exponentially growing away from $r = r_c$, i.e. it is exponentially decaying with radius in $1 < r < r_c$. It therefore matches to the term $b\,\mathrm{e}^{-m\Psi_0 - \Psi_1}$ in the solution in the region $1 < r < r_c$. Correspondingly, the Ai($-a_1^{1/3}x$)-term matches to the solution which is exponentially growing with radius, that is, the term $a\,\mathrm{e}^{m\Psi_0 + \Psi_1}$. Hence by considering (60) and (61) in the limit $z \to \infty$, the ratio of exponentially growing to exponentially decaying terms in the region $1 < r < r_c$ satisfies the relation $a/b = \mathrm{i}/2$. Up to an arbitrary amplitude, therefore, this completes the solution in the range $r > 1$.

5.4. *Region* 4: $0 < r < 1$

In the range $r < 1$, the crucial boundary condition is regularity at $r = 0$. This implies that only solutions of the form

$$v_\theta = d\,\mathrm{e}^{m\Psi_0 + \Psi_1} \tag{65}$$

are possible, where Ψ_0 is given by (62), and Ψ_1 by (63).

5.5. *Jump conditions at* $r = 1$

The final task, which determines the eigenvalue c at successive orders, is to apply continuity of v_r and h at $r = 1$, which is expressed in the continuity condition (19).

To find v_r, we may use to sufficient accuracy

$$\frac{\mathrm{d}v_\theta}{\mathrm{d}r} \sim \frac{\mathrm{i}m}{r} v_r. \tag{66}$$

For $r < 1$, this leads to

$$\left.\frac{v_\theta}{v_r}\right|_{r=1^-} = \mathrm{i} + O(m^{-1}). \tag{67}$$

On the other hand, for $r > 1$, we obtain

$$\frac{v_\theta}{v_r} = \mathrm{i}\frac{\mathrm{e}^{-m\Psi(1)} + \mathrm{i}/2\mathrm{e}^{m\Psi(1)}}{-\mathrm{e}^{-m\Psi(1)} + \mathrm{i}/2\,\mathrm{e}^{m\Psi(1)}}, \tag{68}$$

where here

$$\Psi(1) = \Psi_0(1) + m^{-1}\Psi_1(1). \tag{69}$$

Recalling that $\Psi < 0$, this takes the asymptotic form for large m:

$$\frac{v_\theta}{v_r} \sim \frac{\mathrm{i}}{r\Psi_0'}(1 + \mathrm{i}\,\mathrm{e}^{2m\Psi(1)}). \tag{70}$$

There are algebraic corrections to these terms, but because of our judicious decomposition of A and ψ, (70) expresses the principal exponential terms. In particular, then, it has the correct expression for the leading-order (exponentially small) imaginary part of v_θ/v_r.

Returning to the continuity condition (19), at $O(m)$, we simply have

$$c_0 = \bar{v}(1). \tag{71}$$

At the next order, we obtain

$$c_1 = -\tfrac{1}{2}H_1(1 - \tfrac{1}{2}\mathrm{i}\,\mathrm{e}^{2m\Psi(1)}), \tag{72}$$

where $H_1 = 1 + F^2\bar{h}(1)$.

There are three things to note about (72). Firstly, the correction to the real phase speed of the disturbance is negative, and is in accordance with Kelvin's expression (34) in the limit $F \ll 1$. This is consistent with the claim that the disturbance on the boundary of the vortex has locally the character of a Rossby wave, with a pseudo-westward phase speed. The second thing is that the imaginary correction to c is always positive, corresponding to a temporally growing disturbance of form $\mathrm{e}^{-\mathrm{i}mct}$ at any value of F or f. The growth rate is exponentially small in m, consistent with the expression found using energy conservation arguments by Papaloizou & Pringle (1987) for a different form of basic state. Since the asymptotic limit in this case is of a particular type of disturbance (i.e. large m), rather than a particular type of basic state, as it was in the $F \ll 1$ analysis of §3, we conclude that all basic states which satisfy the assumption of a single turning point are unstable, at least to large-mode-number disturbances. Finally, it can be shown by standard analytical methods that the expressions for the growth rate of the instability in the limits $m \gg 1$ (72) and $F \ll 1$ (44) agree in the joint limit $m \gg 1$ and $F \ll 1$.

5.6. *Comparison with numerical eigenvalue calculations*

In addition to comparison with the analysis in the low-Froude-number limit, we can also test the validity of the general expression (72) given for the growth rate of the instability in the WKBJ limit against the numerical eigenvalue calculations. Growth

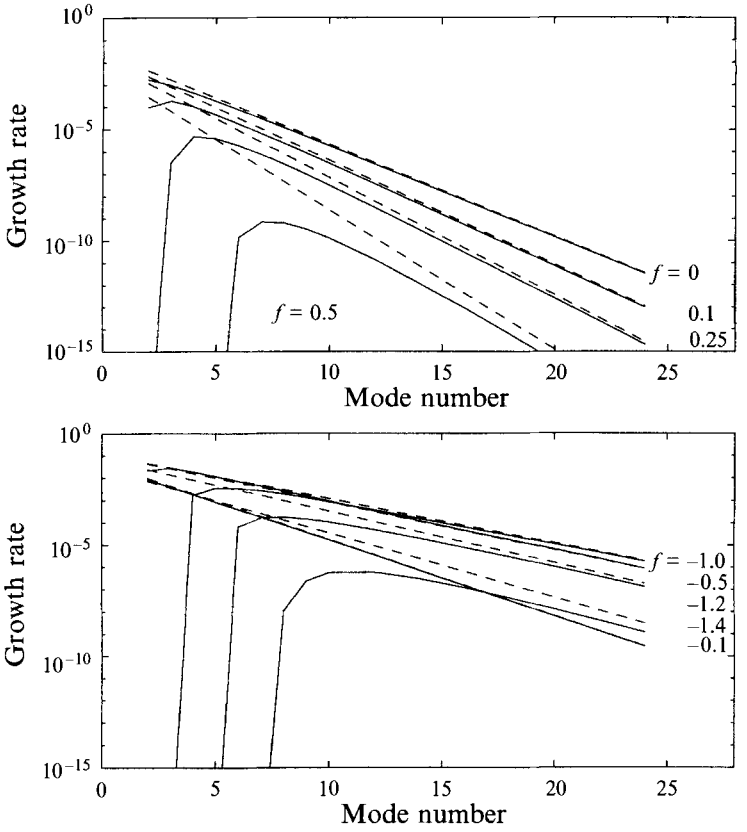

FIGURE 11. Comparison of eigenmode growth rates (solid lines) with WKBJ predictions (dashed lines), $F = 2.5$, for $m = 0$ to 25, at various values of f.

rates of the instability against mode number are shown in figures 11 and 12. The basic states chosen all have Froude number $F = 2.5$ in figure 11, and $F = 5$ in figure 12, with varying values of f indicated on the graphs. Overall there seems to be good agreement between the WKBJ analysis (dashed lines) and the numerical eigenvalue code (solid lines), even for quite moderate values of m.

A significant distinction is to be drawn between $f > 0$ and $f < 0$. For given F, the magnitudes of $\Psi_0(1)$ and $\Psi_1(1)$ are always greater when $f > 0$ than when $f < 0$. It follows immediately that the instability will be weaker for $f > 0$ in the limit of large m. This is significant, in that it is dependent entirely upon the nature of the basic state, and independent of the effects of inertial cut-off, which are assumed not to apply, since the WKBJ analysis assumes that f is of order unity, whereas ω is of order $m \gg 1$. Where the numerical eigenvalues are in good qualitative agreement with the WKBJ prediction, any differences between them for different values of f must be directly attributable to the nature of the basic state alone, and independent of the effects of the inertial cut-off.

For small m and small $|f|$, the eigenmodes are unstable, and their growth rates are broadly in line with the values predicted by the WKBJ analysis. However, as $|f|$ is increased, the eigenmodes become stable at small m. Since this effect is not predicted by the WKBJ analysis, it must be because the eigenfrequencies are comparable with the magnitudes of the inertial frequency, and hence the inertial cut-off is significant.

As a heuristic way of thinking about the behaviour of the growth rates, I propose

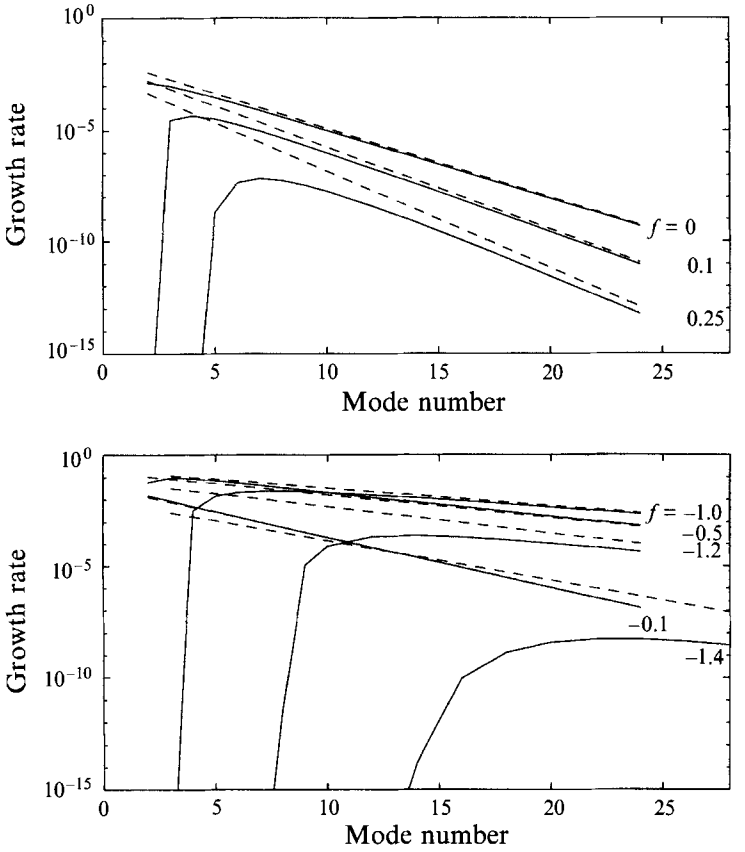

FIGURE 12. Comparison of eigenmode growth rates (solid lines) with WKBJ predictions (dashed lines), $F = 5.0$, for $m = 0$ to 25.

that in the region where they are seen to be increasing with increasing m, it is because the real part of the eigenvalue is increasing. The growth rate is therefore dominated by effects of the inertial cut-off. Examination of figures 11 and 12 shows that, once the instability has set in, this range of m tends to be quite small. However, in the range where the growth rate of the instability decreases with m, I propose that the WKBJ analysis is broadly valid in this limit, and the dependence of the growth rate of the instability on f is determined largely by the nature of induced basic state, and not directly by the effect of the inertial cut-off. Even in the range where the inertial cut-off is dominating the lower eigenmodes, the nature of the basic state is clearly important, in that it sets the real part of the eigenfrequency, and hence determines whether the eigenmodes are unstable or not.

In conclusion, the axisymmetric vortex is always unstable, but as F and $|f|$ are increased, larger and larger values of m must be taken to obtain the instability. Almost all the asymmetry between cyclones and anticyclones can be explained in terms of the basic state. At large m, the nature of the basic state determines the strength of Rossby wave–gravity wave interactions, and at small m it determines whether and by how much the real part of the eigenfrequency will exceed $|f|$, and hence how significantly the instability is affected by the inertial cut-off.

6. Discussion

The instability of an axisymmetric vortex with monotonic potential vorticity has been investigated analytically and numerically. When there is a single radial discontinuity in the potential vorticity, the vortex is always unstable at small Froude number, provided the mode number $m > 1+2|f|$, and is always unstable at large mode number m for all values of F and f. Numerical eigenvalue calculations showed that the growth rate of the instability is typically of order 10^{-7} or less, except when $0 \geqslant f \geqslant -1$, and the potential vorticity in the vortex is of the opposite sign to the background value. In a three-dimensional flow, these vortices are subject to inertial instability. Recalling that the vortex rotation time was used to non-dimensionalize the timescale for this analysis, this means that, except in inertially unstable situations, 10^7 vortex rotation times are typically required for one e-folding time of the instability. In typical geophysical applications, vortex rotation times are at least one day (in many cases much more than one day), and hence the instability grows very much more slowly than typical timescales of evolution of the vortical flow, which is likely to distort the vortex significantly on the timescale of several vortex rotation times. In the case $-1 < f < 0$, where the present instability is strongest, inertial instability also exists in the three-dimensional case, and it was shown that inertial instability is generally stronger than the present instability, except near $f = 0$ and -1, where the present instability is quite weak. The present instability is therefore unlikely to be of any practical interest in geophysical fluid dynamics. On the other hand, the destabilization of cyclones and stabilization of anticyclones in the presence of planetary Rossby wave radiation (the β-effect), is likely to be a much more significant factor than the present instability. This phenomenon is often invoked to explain the persistence of anticyclones over cyclones in the Jovian atmosphere (Nezlin & Snezhkin 1993).

The WKBJ analysis of § 5 elucidates the mechanism of the instability. Disturbances of small amplitude to the boundary of the vortex have retrograde phase progression, consistent with their being regarded as Rossby waves on the vortex boundary. The amplitude of the eigenfunction associated with the Rossby wave at the vortex boundary decays exponentially with radius both inward towards the vortex centre and outward to infinity. However, at a critical radius, the eigenfunction changes from being exponentially decaying to oscillatory, and this implies that the Rossby wave on the vortex boundary is coupled, exponentially weakly, to a gravity wave beyond the critical radius. The gravity waves must also decay exponentially with radius, but much more gradually than the decay betwen the vortex boundary and the critical radius. Moreover, if the imaginary part of the eigenfrequency is small compared with the real part, the condition of exponential decay of the eigenfunction beyond the critical radius is equivalent to imposing an outward radiation condition on the gravity waves which would be obtained by considering only the real part of the eigenfrequency. Consequently, we may regard the instability as due to a coupling between a Rossby wave on the vortex boundary and a gravity wave beyond the critical radius. For a review of instability theory in terms of coupling between different wave modes, see Sakai (1989).

In a provocative paper, Leith (1980) introduced the concept of a 'slow manifold' for the shallow-water equations. The slow manifold, if it exists, is an invariant sub-manifold of the shallow-water equations, of one-third the dimension of the phase space of the shallow-water equations, and tangent to the quasi-geostrophic manifold at zero Rossby number. Moreover, on the slow manifold, the entire velocity field and the entire height field at any instaant in time can be uniquely determined from the potential

vorticity distribution at that instant in time. Under the assumption of linearized perturbations to an axisymmetric vortex, it is straightforward to see that, if the potential vorticity distribution determines the entire velocity and height fields, a perturbation to the boundary of the form of a single azimuthal mode number disturbance must give rise to motion in the form of an eigenmode of the vortex. Now we know that, in unbounded shallow water with constant f, two bounded eigenmodes exist – one temporally growing mode and one temporally decaying mode. Moreover, it can be shown that if one choice is assumed to lie on the slow manifold, then the other will lie on another slow manifold, and that both slow manifolds will contain some gravity-wave-like structures in the tails of the eigenmodes beyond the critical radius. We conclude that the concept of a slow manifold for the shallow-water equations is inherently non-unique, and that it cannot be truly slow, in that it must contain gravity-wave-like structures, albeit at exponentially small amplitude at small Rossby number.

Note that, if it had turned out that the instability did not exist at very small Rossby number, then the temporally growing and temporally decaying modes would coalesce, and would not contain a gravity-wave-like tail. In that case, the slow manifold would be unique and truly slow. Thus, the significance of the persistence of the instability at very small growth rates for all non-zero Froude and Rossby numbers is crucial to establishing the non-existence of a unique slow manifold, or a slow manifold devoid of all gravity-wave-like motion. These ideas are expounded in greater detail in Ford (1993), and Ford, McIntyre & Norton (1994).

This work was carried out while the author was a PhD student, supported by a studentship from the United Kingdom Natural Environment Research Council. The WKBJ analysis was stimulated by discussions with Professor J. B. Keller and Professor G. R. Flierl, while the author was a fellow at the Woods Hole Summer Program in Geophysical Fluid Dynamics, which is supported by a grant from the United States National Science Foundation. Professor M. E. McIntyre made several helpful suggestions as the work progressed, and Dr D. G. H. Tan and an anonymous reviewer suggested several improvements to the manuscript.

Appendix A. Numerical solution of the equations for the basic state

We consider first the singular point $r = \infty$. In this limit, we will impose conditions that $\bar{v}$ and $\bar{h}$ tend to zero as $r \to \infty$. By manipulation of (8) and (9), one obtains

$$\frac{\mathrm{d}^2\bar{h}}{\mathrm{d}r^2} + \frac{1}{r}\frac{\mathrm{d}\bar{h}}{\mathrm{d}r} - F^2 f^2 \bar{h} = \frac{2\bar{v}}{r}\frac{\mathrm{d}\bar{v}}{\mathrm{d}r}, \tag{A 1}$$

$$\frac{\mathrm{d}^2\bar{v}}{\mathrm{d}r^2} + \frac{1}{r}\frac{\mathrm{d}\bar{v}}{\mathrm{d}r} - \left(F^2 f^2 + \frac{1}{r^2}\right)\bar{v} = F^2 f \frac{\bar{v}^2}{r}. \tag{A 2}$$

Imposing evanescence conditions as $r \to \infty$, we note that the nonlinear right-hand sides of (A 1) and (A 2) will be of small order compared with $\bar{v}$ and $\bar{h}$ in the limit $r \to \infty$. A convenient form of solution for $r \to \infty$ is therefore

$$\bar{h} = \mathrm{K}_0(\alpha r)\, \boldsymbol{H}(r), \tag{A 3}$$

$$\bar{v} = \mathrm{K}_1(\alpha r)\, \boldsymbol{V}(r), \tag{A 4}$$

where $\boldsymbol{H}(r)$ and $\boldsymbol{V}(r)$ tend to some finite non-zero limits $\boldsymbol{H}_\infty$ and $\boldsymbol{V}_\infty$ respectively as

$r \to \infty$, and $\alpha = F|f|$ is the Rossby deformation radius for this problem. Differential equations for $\boldsymbol{H}$ and $\boldsymbol{V}$ are

$$\frac{d\boldsymbol{V}}{dr} = \frac{K_0(\alpha r)}{K_1(\alpha r)}(\alpha \boldsymbol{V} + F^2 f \boldsymbol{H}), \tag{A 5}$$

$$\frac{d\boldsymbol{H}}{dr} = \frac{K_1(\alpha r)}{K_0(\alpha r)}\left(f\boldsymbol{V} + \alpha \boldsymbol{H} + \frac{K_1(\alpha r)}{r}\boldsymbol{V}^2\right), \tag{A 6}$$

from which it follows that

$$\boldsymbol{V}_\infty = -\frac{\alpha}{f}\boldsymbol{H}_\infty. \tag{A 7}$$

Then, given an initial estimate for $\boldsymbol{H}_\infty$, and taking some $R \gg \alpha^{-1}$, we take $\boldsymbol{H} = \boldsymbol{H}_\infty$ at $r = R$, and (A 7) as the relationship between $\boldsymbol{H}$ and $\boldsymbol{V}$ at $r = R$. We can then integrate (A 5) and (A 6) backwards to the boundary of the vortex.

The sole exception is in the case $f = 0$, where the form of the solution for $\bar{v}$ is known outside the vortex boundary:

$$\bar{v} = A/r; \quad \bar{h} = -A^2/(2r^2), \tag{A 8}$$

where A is an arbitrary constant, and hence for $r > 1$, $\bar{v}$ and $\bar{h}$ are known in terms of the constant A rather than the constant $\boldsymbol{H}_\infty$.

In the vicinity of $r = 0$, $\bar{h} \sim O(1)$ and $\bar{v} \sim O(r)$ as $r \to 0$. In this case, simple power series expansions in r of the form

$$\bar{h}(r) = h_0 + h_2 r^2 + h_4 r^4 + h_6 r^6 + \ldots, \tag{A 9}$$

$$\bar{v}(r) = v_1 r + v_3 r^3 + v_5 r^5 + v_7 r^7 + \ldots \tag{A 10}$$

are sufficient to give $\bar{h}(r)$ and $\bar{v}(r)$ at some small, non-zero r, given a guess h_0 for $h(0)$. We can then integrate (8) and (9) forwards in r to the boundary of the vortex.

At the boundary of the vortex, we impose continuity of $\bar{h}$ and $\bar{v}$. A Newtonian method was used to iterate on h_0 and $\boldsymbol{H}_\infty$ (and h_0 and A in the case of $f = 0$) until the discontinuities in $\bar{h}$ and $\bar{v}$ across the boundary fell below some prescribed tolerance. To employ a Newton method, the differential equations (8), (9), (A 5) and (A 6) and the starting series (A 7), (A 9) (A 10) were differentiated with respect to the parameters h_0 and $\boldsymbol{H}_\infty$, so that the variation of $\bar{v}$ and $\bar{h}$ with respect to h_0 and $\boldsymbol{H}_\infty$ on either side of the vortex boundary could be obtained (in the case $f = 0$, it is trivial to obtain expressions for the derivatives of the boundary velocity and height with respect to A). For $F \ll 1$, good initial guesses for h_0 and $\boldsymbol{H}_\infty$ or A were obtained from a matched asymptotic analysis, with h_0 given by C_1 due to (22) and (28), and $\boldsymbol{H}_\infty = -\frac{1}{2}f$ due to (25), or $A = \frac{1}{2}$.

Appendix B. Numerical solution of the eigenvalue problem

We start by considering the limit $r \to 0$. Here, we may take $v_r = r^{m-1} + k_1 r^{m+1} + \ldots$. Regularity at $r = 0$ then implies that $v_\theta = \mathrm{i}r^{m-1} + k_2 r^{m+1} + \ldots$. The constants k_1 and k_2 can then be obtained from the eigenvalue equations, and

$$v_r/v_\theta = -\mathrm{i} + K_2 r^2 + O(r^4). \tag{B 1}$$

The constant K_2 depends on the eigenvalue ω. Hence, given an initial guess for ω, the ratio of v_r to v_θ is known in the limit $r \to 0$ from the series (B 1). The ratio is used to

initialize the r-integration of the eigenvalue equations with a starting value of $r = 10^{-4}$, and in all eigenvalue calculations the starting series (83) was terminated at $O(r^2)$. The first neglected term is of order r^4, so the error involved here is of order 10^{-16}. Using this procedure, the ratio v_r/v_θ is thus known just inside the vortex boundary.†

In the limit $r \to \infty$, since the background flow is exponentially small there, we have

$$h \sim H_m^{(1)}(\lambda r) \tag{B 2}$$

with exponentially small corrections, where

$$\lambda^2 = (\omega^2 - f^2) F^2, \tag{B 3}$$

and the type of the Hankel function is chosen to satisfy the radiation condition. Rearranging (10), (11) and (12) we have a relationship between v_r and v_θ through

$$(f^2 - \omega^2) v_r + \mathrm{i}\omega \frac{\mathrm{d}h}{\mathrm{d}r} + \frac{1}{r} \mathrm{i} m f h = 0, \tag{B 4}$$

$$(f^2 - \omega^2) v_\theta - f \frac{\mathrm{d}h}{\mathrm{d}r} - \frac{1}{r} m \omega h = 0. \tag{B 5}$$

In the case where $\omega^2 \sim f^2$ we can still find a non-singular expression for the ratio v_r/v_θ by expanding the Hankel function representation of h. Again, the amplitude of h is not important – it is sufficient to know the ratio of the velocities v_r/v_θ.

Note that there is no need to integrate the disturbance equations in from the radiation far field of the Hankel function. This is fortunate, since, if $\omega^2 \sim f^2$, this would require a very large range of integration indeed. Equations (B 4) and (B 5) assume negligible basic-state velocity and perturbation height fields, but not a far-field form of the wave field. Therefore, it is sufficient to integrate in from a radius where the departure of the basic state from a resting layer of uniform depth is sufficiently small. In all cases shown here, the integration was from a point at which $\bar{v}$ and $\bar{h}$ were less than 10^{-15}. Since the decay rate of the basic state with r is indepdneent of the eigenvalue, the required outer limit of the integration for the eigenfunction equations in the region $r > 1$ is fixed for given F and $|f|$, and decreases as F and $|f|$ increase.

Given an initial guess for ω, we must iterate on ω to satisfy the continuity equation (19). Here it is not so convenient to use a Newton method, owing to the non-analytic behaviour of the solution at $\omega = \pm f$. However, iteration from two initial guesses using linear interpolation to predict the location of the root was found to perform reasonably well, typically converging in 5 or 6 iterations.

At low Froude number, we supply an initial guess for ω by considering the Kelvin modes on a circular incompressible vortex, with frequency given by (34). This can be used as a first guess ω_0 for the eigenfrequency, and a second guess can be supplied which is not too far away ($\omega_0 - 0.05$, say).

At low Froude number, growth rates are typically very low, and this places a strain on the numerical accuracy required. In all cases presented here, NAG routines were used for integrating the ODEs for both the basic-state problem and the eigenvalue problem, using double-precision arithmetic. In the exterior of the vortex, the differential equations are stiff, and a backward differencing method was used. A forward differencing method was used for the interior of the vortex. Tolerances of 10^{-15} were specified in all numerical integrations. In the disturbance problem, the computational

† I thank an anonymous reviewer for pointing out that the starting value of r was taken to be too large for consistency with other error estimates in an earlier version of the paper.

values of the eigenfunctions were kept of order unity throughout the ranges of integration by applying the scaling function $(1+(Fr)^{2m})^{-1}r^{-1/2}\mathrm{e}^{-\lambda_r r}$ to the variables in the exterior of the vortex (where λ_r is the real part of λ, and λ is given by (B 3)), and the function r^{m-1} to the interior variables. The very low tolerance specification, together with the rescaling to make the computational variables of order unity throughout the domains of integration, and starting integrations from sufficiently small and large r that errors involved are of order 10^{-15} means that we can have some confidence in the imaginary parts of the eigenvalues down to around 10^{-14}, although a rigorous analysis of the cumulative error has not been attempted.

Appendix C. Inertial instability

In this appendix, we derive the conditions for an axisymmetric vortex on an f-plane to be inertially unstable, and obtain an expression for the maximum growth rate of the instability.

We have been studying vortices with uniform potential vorticity in the shallow-water equations. The definition of potential vorticity must be modified to apply to the continuously stratified case, and the velocity and height/pressure fields which we have found for axisymmetric vortices in shallow water will not necessarily correspond to vortices with uniform potential vorticity in a continuously stratified system. In general, solution of the hydrostatic equations for axisymmetric vortices with specified potential vorticity requires considerable effort (Thorne 1985). However, for the purposes of the present discussion, we are concerned with approximate estimates of the growth rate of inertial instability. Therefore, we shall take the same velocity field as in the shallow-water equations, identify the height field in the shallow-water equations with the pressure in the stratified fluid equations, and compute the growth rates of inertial instability for a Boussinesq fluid with uniform buoyancy frequency N^2 and a basic state independent of height.

We consider a Boussinesq hydrostatic fluid with constant buoyancy frequency N^2. Assuming linear disturbances of form $f(r)\mathrm{e}^{\mathrm{i}(nz-\omega t)}$, the disturbance equations are

$$-\mathrm{i}\omega v_r-(f+2\bar{v}/r)+\mathrm{d}p/\mathrm{d}r=0, \tag{C 1}$$

$$-\mathrm{i}\omega v_\theta+(f+\mathrm{d}\bar{v}/\mathrm{d}r+\bar{v}/r)=0, \tag{C 2}$$

$$\mathrm{i}np-\theta=0, \tag{C 3}$$

$$(1/r)(\mathrm{d}/\mathrm{d}r)(rv_r)+\mathrm{i}nw=0, \tag{C 4}$$

$$-\mathrm{i}\omega\theta+N^2w=0, \tag{C 5}$$

where here p is the pressure, w is the vertical velocity, θ is the buoyancy, and all other symbols are as previously defined.

After re-arranging to obtain a single disturbance equation for v_r, we have

$$\frac{1}{r}\frac{\mathrm{d}}{\mathrm{d}r}\left(r\frac{\mathrm{d}v_r}{\mathrm{d}r}\right)-\left[\frac{1}{r^2}+\left(f+2\frac{\bar{v}}{r}\right)\left(f+\frac{\mathrm{d}\bar{v}}{\mathrm{d}r}+\frac{\bar{v}}{r}\right)\frac{n^2}{N^2}\right]v_r=-\omega^2\frac{n^2}{N^2}v_r. \tag{C 6}$$

Using standard techniques, it can be shown that

$$\omega^2_{min}=\frac{\displaystyle\int r\frac{N^2}{n^2}\left|\frac{\mathrm{d}v_r}{\mathrm{d}r}\right|^2+\left[\frac{N^2}{n^2r^2}+\left(f+2\frac{\bar{v}}{r}\right)\left(f+\frac{\mathrm{d}V}{\mathrm{d}r}+\frac{V}{r}\right)\right]r|v_r|^2}{\displaystyle\int r|v_r|^2}. \tag{C 7}$$

Thus, $\omega^2 > 0$, and linear stability is assured, if

$$\left(f+2\frac{\bar{v}}{r}\right)\left(f+\frac{\mathrm{d}\bar{v}}{\mathrm{d}r}+\frac{\bar{v}}{r}\right) > 0 \quad \text{for all} \quad r. \tag{C 8}$$

On the other hand, if $(f+2\bar{v}/r)(f+\mathrm{d}\bar{v}/\mathrm{d}r+\bar{v}/r) < 0$ somewhere in the domain, at $r = r_i$, say, we consider the test function which is unity at $r = r_i$ and zero everywhere else, except over a range of order ϵ, where the test function varies from 0 to 1 or from 1 to 0. Then, by making the vertical wavenumber n large compared with ϵ^{-1}, we have

$$\omega^2_{min} = \mathrm{Min}\left(f+2\frac{\bar{v}}{r}\right)\left(f+\frac{\mathrm{d}\bar{v}}{\mathrm{d}r}+\frac{\bar{v}}{r}\right) < 0 \tag{C 9}$$

and hence we can obtain the maximum growth rate of the instability.

REFERENCES

ABRAMOWITZ, M. & STEGUN, I. A. 1965 *Handbook of Mathematical Functions*. Dover.

BROADBENT, E. G. & MOORE, D. W. 1979 Acoustic destabilisation of vortices. *Phil. Trans. R. Soc. Lond.* A **290**, 353–371.

CARNEVALE, G. F., MCWILLIAMS, J. C., POMEAU, Y., WEISS, J. B. & YOUNG, W. R. 1991 Evolution of vortex statistics in two-dimensional turbulence. *Phys. Rev. Lett.* **66**, 2735–2737.

CROW, S. C. 1970 Aerodynamic sound generation as a singular perturbation problem. *Stud. Appl. Maths* **49**, 21–44.

DRITSCHEL, D. G. 1988 Nonlinear stability bounds for inviscid, two-dimensional, parallel or circular flows with monotonic vorticity, and the analogous three-dimensional quasi-geostrophic flows. *J. Fluid Mech.* **191**, 575–581.

DRITSCHEL, D. G. 1993 Vortex properties of two-dimensional turbulence. *Phys. Fluids* A **5**, 173–186.

FORD, R. 1993 Gravity wave generation by vortical flows in a rotating frame. PhD thesis, University of Cambridge.

FORD, R., MCINTYRE, M. E. & NORTON, W. A. 1994 Balance and the slow quasi-manifold: some explicit results. *J. Atmos. Sci.* (to be submitted).

GILL, A. E. 1982 *Atmosphere-Ocean Dynamics*, Academic.

KELVIN, LORD 1880 On the oscillations of a columnar vortex. *Phil. Mag.* **10**, 155–168.

KNESSL, C. & KELLER, J. B. 1992 Stability of rotating shear flows in shallow water. *J. Fluid Mech.* **244**, 605–614.

KOP'EV, V. F. & LEONT'EV, E. A. 1983 Acoustic instability of an axial vortex. *Sov. Phys. Acoust.* **29**, 111–115.

LEGRAS, B. & DRITSCHEL, D. G. 1993 Vortex stripping and the generation of high vorticity gradients in two-dimensional flows. In *Advances in Turbulence IV* (ed. F. T. M. Nieuwstadt). Kluwer.

LEGRAS, B., SANTANGELO, P. & BENZI, R. 1988 High-resolution numerical experiments for forced two-dimensional turbulence. *Europhys. Lett.* **5**, 37–42.

LEITH, C. E. 1980 Non-linear normal mode initialization and quasi-geostrophic theory *J. Atmos. Sci.* **37**, 958–968.

LIGHTHILL, M. J. 1952 On sound generated aerodynamically, I. General theory. *Proc. R. Soc. Lond.* A **211**, 564–587.

NEZLIN, M. V. & SNEZHKIN, E. N. 1993 *Rossby Vortices, Spiral Structures, Solitons: Astrophysics and Plasma Physics in Shallow Water Experiments*. Springer.

OOYAMA, K. 1966 On the stability of the baroclinic circular vortex: a sufficient criterion for instability. *J. Atmos. Sci.* **23**, 43–53.

PAPALOIZOU, J. C. B. & PRINGLE, J. B. 1984 The dynamic stability of differentially rotating discs with constant specific angular momentum. *Mon. Not. R. Astron. Soc.* **208**, 721–750.

PAPALOIZOU, J. C. B. & PRINGLE, J. B. 1985 The dynamic stability of differentially rotating discs: II. *Mon. Not. R. Astron. Soc.* **213**, 799–820.

PAPALOIZOU, J. C. B. & PRINGLE, J. B. 1987 The dynamic stability of differentially rotating discs: III. *Mon. Not. R. Astron. Soc.* **225**, 267–283.

POLVANI, L. M., MCWILLIAMS, J. C., SPALL, M. A. & FORD, R. 1994 The coherent structures of shallow-water turbulence: deformation radius effects, cyclone/anticyclone asymmetry and gravity-wave generation. *Chaos* **4**, 177–186.

RIPA, P. 1987 On the stability of elliptical vortex solutions of the shallow water equations. *J. Fluid Mech.* **183**, 343–363.

SAKAI, S. 1989 Rossby–Kelvin instability: a new type of ageostrophic instability caused by resonance between Rossby waves and gravity waves. *J. Fluid Mech.* **202**, 149–176.

SHUKHMAN, I. G. 1991 Nonlinear evolution of spiral density waves generated by the instability of the shear layer in a rotating compressible fluid. *J. Fluid Mech.* **233**, 587–612.

SOZOU, C. 1987 New solutions representing adiabatic transverse waves in a Rankine vortex. *Proc. R. Soc. Lond.* A **413**, 225–234.

THORPE, A. J. 1985 Diagnosis of balanced vortex structure using potential vorticity. *J. Atmos. Sci.* **42**, 397–406.

WILLIAMS, J. S. 1992 Nonlinear problems in vortex sound. PhD thesis, University of Leeds.